NTIS # PB2013-

SSC-466

MEAN STRESS ASSESSMEN IN FATIGUE ANALYSIS AND DESIGN

This document has been approved
For public release and sale; its
Distribution is unlimited

SHIP STRUCTURE COMMITTEE
2013

Ship Structure Committee

RDML J.A. Servidio
U. S. Coast Guard Assistant Commandant,
Assistant Commandant for Prevention Policy
Co-Chair, Ship Structure Committee

RADM Thomas Eccles
Chief Engineer and Deputy Commander
For Naval Systems Engineering (SEA05)
Co-Chair, Ship Structure Committee

Mr. H. Paul Cojeen
Society of Naval Architects and Marine Engineers

Mr. Todd Grove
Chief Technical Officer (CTO)
American Bureau of Shipping

Mr. Christopher McMahon
Director, Office of Ship Construction
Maritime Administration

Ms. Julie Gascon
Director Design, Equipment and Boating Safety,
Marine Safety,
Transport Canada

Mr. Kevin Baetsen
Director of Engineering
Military Sealift Command

Dr. Neil Pegg
Group Leader - Structural Mechanics
Defence Research & Development Canada - Atlantic

Mr. Jeffrey Lantz,
Commercial Regulations and Standards for the
Assistant Commandant for Marine Safety, Security
and Stewardship
Mr.
Deputy Assistant Commandant for Engineering and
Logistics

Mr. Eric C. Duncan
Director, Structural Integrity and Performance Division

Dr. John Pazik
Director, Ship Systems and Engineering Research
Division

SHIP STRUCTURE SUB-COMMITTEE

AMERICAN BUREAU OF SHIPPING (ABS)

Mr. Craig Bone
Mr. Phil Rynn
Mr. Tom Ingram

DEFENCE RESEARCH & DEVELOPMENT CANADA ATLANTIC

Mr. Malcolm Smith
Dr. Layton Gilroy

MARITIME ADMINISTRATION (MARAD)

Mr. Chao Lin
Mr. Richard Sonnenschein

MILITARY SEALIFT COMMAND (MSC)

Mr. Michael W. Touma
Mr. Jitesh Kerai

NAVY/ONR / NAVSEA/ NSWCCD

Mr. David Qualley / Dr. Paul Hess
Mr. Erik Rasmussen / Dr. Roshdy Barsoum
Mr. Nat Nappi, Jr.
Mr. Dean Schleicher

TRANSPORT CANADA

Mr. Ian Campbell
Mr. Bashir Ahmed Golam
Mr. Luc Tremblay

UNITED STATES COAST GUARD

CAPT John Mauger
Mr. Jaideep Sirkar
Mr. Chris Cleary
Mr. Frank DeBord

SOCIETY OF NAVAL ARCHITECTS AND MARINE ENGINEERS (SNAME)

Mr. Rick Ashcroft
Mr. Dave Helgerson
Mr. Alex Landsburg
Mr. Paul H. Miller

Member Agencies:

American Bureau of Shipping
Defence Research and Development Canada
Maritime Administration
Military Sealift Command
Naval Sea Systems Command
Office of Naval Research
Society of Naval Architects & Marine Engineers
Transport Canada
United States Coast Guard

Ship Structure Committee

Address Correspondence to:

COMMANDANT (CG-ENG-2/SSC)
ATTN (EXECUTIVE DIRECTOR/SHIP STRUCTURE COMMITTEE)
US COAST GUARD
2100 2ND ST SW STOP 7126
WASHINGTON DC 20593-7126
Website: http://www.shipstructure.org

SSC – 466
SR – 1458

June 28, 2013

MEAN STRESS ASSESSMENT IN FATIGUE ANALYSIS AND DESIGN

Understanding the mean stresses and fatigue strength of ship structures is important in determining the overall strength of a vessel throughout its service life. However, there are numerous methods used in conducting a fatigue analysis in the design phase of vessels. This lack of commonality between the different approaches in fatigue analysis and design codes and standards makes it necessary to validate models adopted in the various approaches. This project develops a procedure to validate those models and seeks to harmonize the various approaches toward conducting fatigue analyses. These goals are accomplished via an extensive study of the available data on the effects of mean stress on fatigue strength, followed by an analysis of results from actual experiments on structural steel members, resulting in the development of a methodology for assessing the mean stress effects in fatigue analyses for marine applications.

We thank the authors and Project Technical Committee for their dedication and research toward completing the objectives and tasks detailed throughout this paper and continuing the Ship Structure Committee's mission to enhance the safety of life at sea.

JOSEPH A. SERVIDIO
Rear Admiral, U.S. Coast Guard
Co-Chairman, Ship Structure Committee

T. J. ECCLES
Rear Admiral, U.S. Navy
Co-Chairman, Ship Structure Committee

Technical Report Documentation Page

1. Report No.	2. Government Accession No.	3. Recipient's Catalog No.
466		

4. Title and Subtitle	5. Report Date
Mean Stress Assessment in Fatigue Analysis and Design	6. Performing Organization Code
7. Author(s) Yuen, B.K.; Koko T.S.; Polezhayeva; H; Jiang L.	8. Performing Organization Report No. SR-1458
9. Performing Organization Name and Address Martec Limited 1888 Brunswick Street, Suite 400 Halifax, NS Canada B3J 3J8	10. Work Unit No. (TRAIS) 11. Contract or Grant No.
12. Sponsoring Agency Name and Address COMMANDANT (CG-ENG-2/SSC) ATTN (SHIP STRUCTURE COMMITTEE) US COAST GUARD 2100 2ND ST SW STOP 7126 WASHINGTON DC 20593-7126	13. Type of Report Final Report 14. Sponsoring Agency Code CG – 5P

15. Supplementary Notes

The research completed by the above author for the Ship Structure Committee was reviewed by the Project Technical Committee for satisfactory completion of the objectives outlined in the Statement of Work developed and approved for funding by the Principal Members of the Ship Structure Committee.

Sponsored by the Ship Structure Committee and its member agencies

16. Abstract

The mean stress is an important component of loading history and fatigue of ship hull structural details. This is especially true in welded details, where the tensile residual stress at a hot spot is very large and close to the yield stress, which might reduce the fatigue life of structural components. However, there is a lack of commonality between different approaches in fatigue analysis and design codes and standards when dealing with mean stress.

Therefore, the objectives of this work are to validate the models adopted in the various approaches, to seek to harmonize these approaches across the codes and to develop an appropriate methodology for assessing the effects of mean stress. These objectives were accomplished through a review the available data on the effects of mean stress on fatigue strength and the analyses the available fatigue data in order to develop an appropriate methodology for the assessment of the mean stress effects in fatigue analyses for marine applications.

17. Key Words	18. Distribution Statement
mean stress, fatigue models, residual stress, welded details, ships, design codes, and standards	National Technical Information Service U.S. Department of Commerce Springfield, VA 22151 Ph. (703) 487-4650 / www.ntis.gov

19. Security Classif. (of this report)	20. Security Classif. (of this page)	21. No. of Pages	22. Price
Unclassified	Unclassified		

1. Report No. SSC-XXX	2. Government Accession No.	3. Recipient's Catalog No.
4. Title and Subtitle Mean Stress Assessment in Fatigue Analysis and Design		5. Report Date November 2012
		6. Performing Organization Code
7. Authors Yuen, B.K.; Koko, T.S.; Polezhayeva, H; Jiang, L.		8. Performing Organization Report No.
9. Performing Organization Name and Address Martec Limited 1888 Brunswick Street, Suite 400 Halifax, Nova Scotia Canada B3J 3J8		10. Work Unit No. (TRIAS)
		11. Contract or Grant No.
12. Sponsoring Agency Name and Address		13. Type of Report and Period Covered
		14. Sponsoring Agency Code
15. Supplementary Notes		

16. Abstract

The mean stress is an important component of loading history and fatigue of ship hull structural details. This is especially true in welded details, where the tensile residual stress at a hot spot is very large and close to the yield stress, which might reduce the fatigue life of structural components. However, there is a lack of commonality between different approaches in fatigue analysis and design codes and standards when dealing with mean stress. Therefore, the objectives of this work are to validate the models adopted in the various approaches, to seek to harmonize these approaches across the codes and to develop an appropriate methodology for assessing the effects of mean stress. These objectives were accomplished through a review the available data on the effects of mean stress on fatigue strength and the analyses the available fatigue data in order to develop an appropriate methodology for the assessment of the mean stress effects in fatigue analyses for marine applications.

17. Key Words mean stress, fatigue models, residual stress, welded details, ships, design codes and standards	18. Distribution Statement		
19. Security Classif. of this report	20. Security Classif. of this page	21. No. of pages	22. Price

1.0 INTRODUCTION

1.1 BACKGROUND

The mean stress is an important component of the loading history and fatigue of ship hull structural details. When tensile, it increases the maximum stress in the load cycle and reduces the fatigue life of structural components. The lack of commonality between different approaches in fatigue analysis and design codes and standards when dealing with mean stress makes it necessary to validate the models adopted in the various approaches, and to seek to harmonize these approaches across the codes. However, in the case of the combination of random and constant amplitude loading components, the appropriate methodologies for assessing the effects of mean stress are lacking. A survey carried out in 2003 by ISSC reported that 6 out of 8 major classification societies used a mean stress correction factor. In the recently adopted Common Structural Rules for Tankers and Bulk Carriers (IACS, 2005) mean stress corrections are implemented, albeit in a very different form for tankers and bulk carriers respectively. A procedure for considering mean stress was suggested recently in IACS documents by introducing an equivalent stress, which allows residual welding stress and mean stress due to still water loading to be taken into account. However, application of corrections and of equivalent stress may be regarded only as an approximation since it is based on the simplified assumption of combined cyclic stress with constant amplitude and mean stress.

A specific property of load sequences in marine applications is the combination of a narrow banded random wave loading with slowly varying (or constant) loading providing the source of mean stress. This means that the implied experimental procedure and respective modelling of fatigue behaviour of the material should consider the effects of mean stress in conjunction with realistic variable amplitude loading. An important component of stress fields in a ship structure is residual welding stress. Typically, areas of residual stress are superimposed with the stress concentration due to the geometry of structural details. Static loads and occasionally relatively high wave loads may cause partial relief (shakedown) of residual stress in stress concentration areas, changing the local load ratio and thus affecting fatigue resistance. These effects should be assessed based on the present knowledge and an experimental program, feasible within the framework of the time and cost of the project. These are the reasons for development of a procedure for fatigue analysis and design of marine structural components considering effects of mean stress.

1.2 OBJECTIVES AND SCOPE

The objective of this study is to review the available data on the effects of mean stress on fatigue strength, to plan and carry out additional experiments on a structural steel or steels if necessary, to analyze the results and to develop a methodology for assessment of the mean stress effects in fatigue analyses for marine applications. While both crack initiation and crack growth phases of fatigue analysis are of interest, the objective of this study will be to concentrate on crack initiation.

1.3 ORGANIZATION OF THIS DOCUMENT

The remainder of this document is organized as follows, presenting the literature review on the mean stress effects on fatigue assessment, the development of an appropriate fatigue model to account for the mean stress effects and the analysis of fatigue test data:

- Chapter 2 presents an overview of the effect of mean stress on the fatigue strength of small specimens and components under constant and variable amplitude loading, and when overloads are applied before fatigue tests. Measurements of relaxation of welding residual stresses and hot spot stresses in fatigue critical locations are also discussed. A database of fatigue test results has been developed and this chapter provides a summary of the database. A summary of mean stress models is provided.
- Chapter 3 presents the development of an appropriate fatigue model to account for the mean stress effects. This chapter also includes an analysis of existing fatigue test data using the Class Society and the proposed models.
- Chapter 4 provides a summary of the work performed and conclusions reached. Recommendations for future work are also provided in this chapter.

2.0 LITERATURE REVIEW

2.1 INTRODUCTION

Lloyd's Register (Polezhayeva, 2010) [1] has performed an extensive literature survey on the effect of mean stress on fatigue strength on welded joints. Over 59 published documents were reviewed in the report. Topics that were covered include:

- Effect of mean stress on fatigue strength of small specimens and structural components under constant and variable amplitude fatigue loading;
- Effect of mean stress on fatigue strength of small specimens and structural components under fatigue loading when an overload is applied before the fatigue tests;
- Measurements of relaxation of welding residual stress.

A summary of the review is presented in this chapter, along with reviews of recent experimental investigations into fatigue life of small specimens and structural components, conducted at Lloyd's Register (Polezhayeva, 2010) [2], and hot spot stresses at fatigue critical locations due to static loads.

2.2 EFFECT OF MEAN STRESS ON FATIGUE STRENGTH OF SMALL SPECIMENS AND COMPONENTS UNDER CONSTANT AND VARIABLE AMPLITUDE LOADING

Maddox (1982) [3] tested fillet welded joints in four steels with yield stresses ranging from 332 to 727 MPa, under various applied stress ratios. Some specimens were stress-relieved. The specimen dimensions are provided in Figure 1.

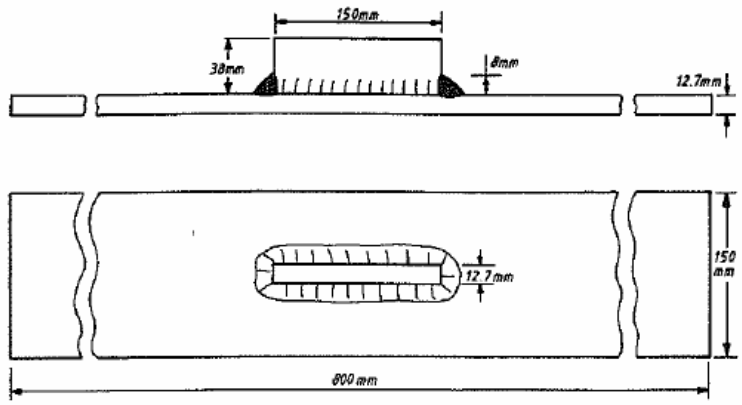

Figure 1: The specimen dimensions in [3]

The specimens were tested axially under constant amplitude stress range and a number of *R*-values, $R = -\infty$, -1, 0, 0.5, 0.67 for as welded specimens and R = -1, 0.5, 0.67 for stress relieved specimens. Experimental data and mean S-N curves are presented in Figure 2. If one defines a fatigue enhancement factor (*f*) as the ratio of the fatigue strength for partially or fully compressive fatigue cycles to the fatigue strength for fully tensile fatigue cycles:

$$f = S_{R<0} / S_0 \tag{1}$$

where S_0 is the fatigue strength when the stress ratio is equal to 0 (entirely tensile fatigue cycles) and $S_{R<0}$ is the fatigue strength when the stress ratio is less than 0 (partly compressive fatigue cycles), then the fatigue enhancement factor for specimens tested under fully compressive cycles was 1.22. Tensile strength of the steel had no effect on the fatigue strength of joints. Stress relief was only partially effective, with the result that applied compressive stresses were still damaging. Stress relief had no effect on the fatigue strength of the joint when it was subjected to tensile loading.

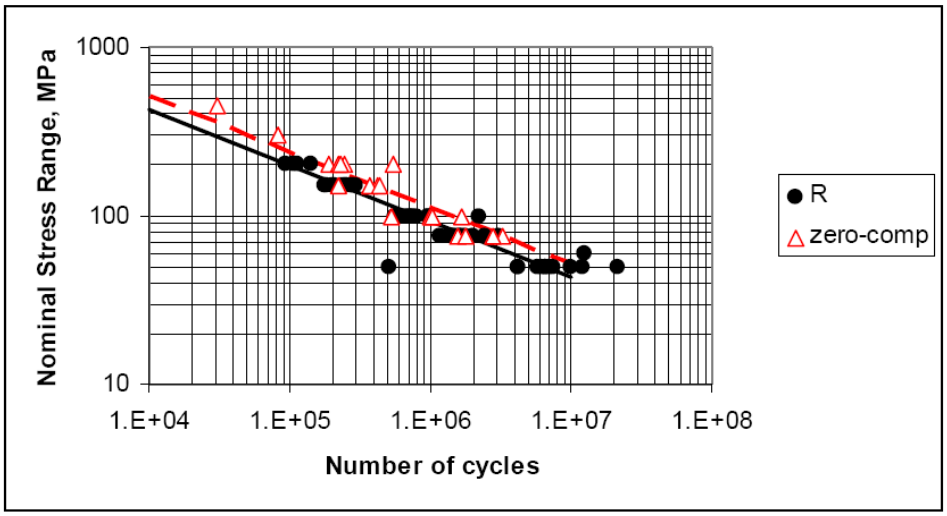

Figure 2: Fatigue test results in [3]

Maddox [4] carried out fatigue tests on longitudinal fillet welded specimens, as shown in Figure 3, in Al-Zn-Mg alloy. Specimens were tested axially: Type 1 with $R = 0$, -1 and -∞; Type 2 with R = -1 and 0.25. Fatigue tests results are shown in Figure 4 for Type 1 specimens. Tests showed the fatigue enhancement factor for specimens tested under fully compressive cycles was 1.57, compared with those tested under tensile and partly compressive stress cycles.

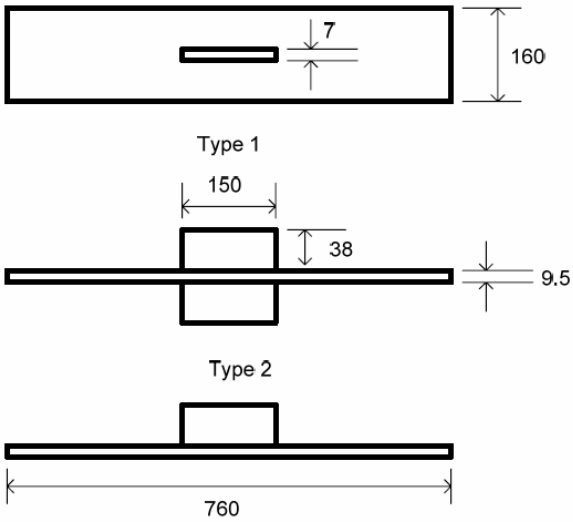

Figure 3: Specimens tested in [4]

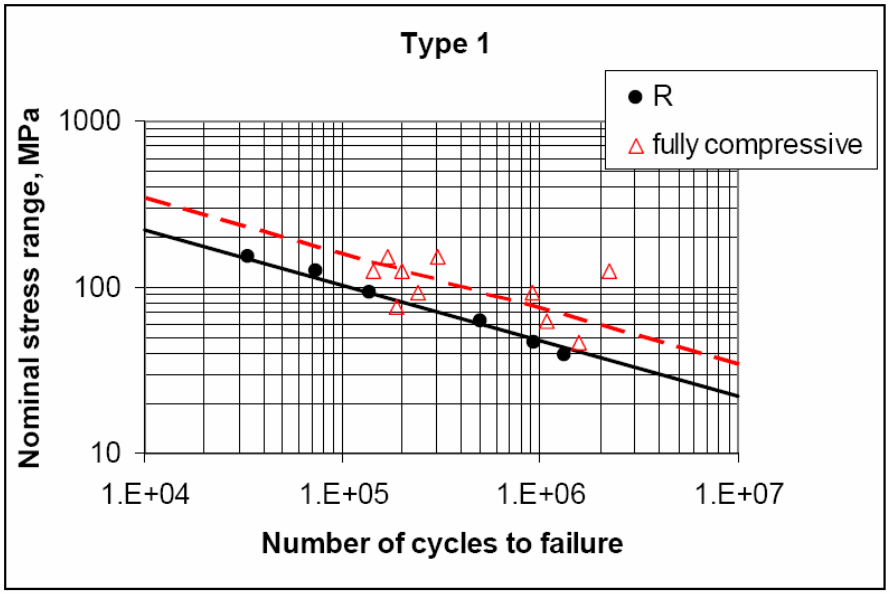

Figure 4: Fatigue test results for Type 1 specimens in [4]

Tilly (1985) [5] stated that under constant amplitude loading, data for pulsating compression (compressive fatigue cycles) tend to be more scattered but the lower limit to performance is a little better than for tension, as shown in Figure 5. Unlike pulsating tension (tensile fatigue cycles), the rate of propagation decreases during the life but does not decay to zero.

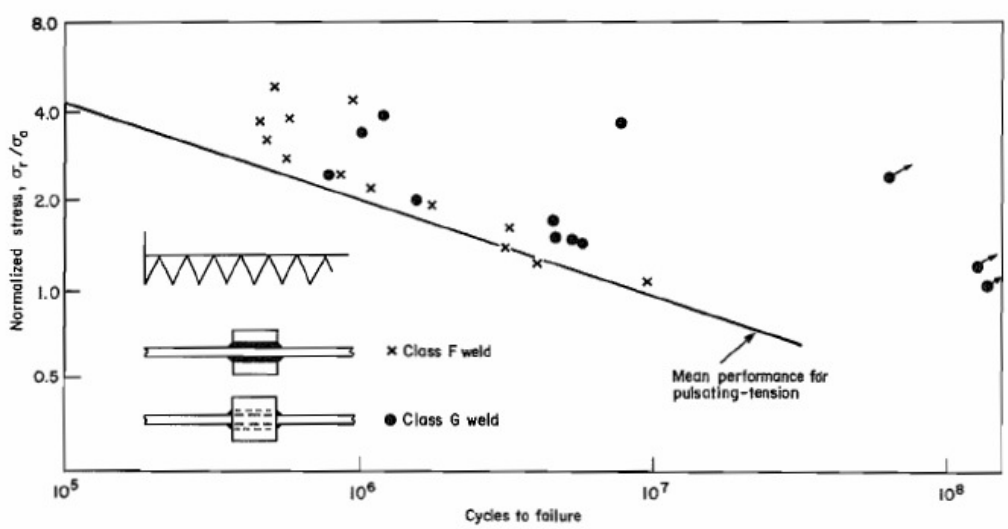

Figure 5: Fatigue test results in [5]

Figure 6 shows fatigue test data conducted with variable amplitude pulsating compression, obtained under a Raleigh spectrum and an axle spectrum, which is the total weight felt by the roadway for all wheels connected to a given axle of a wheeled vehicle. In both cases, results were reasonably close to the performance predicted from pulsating tension data but short of expectation based on constant amplitude pulsating compression

tests, although there were still higher fatigue lives under pulsating compression. Variable amplitude pulsating compression, however, is not typical for ship structures.

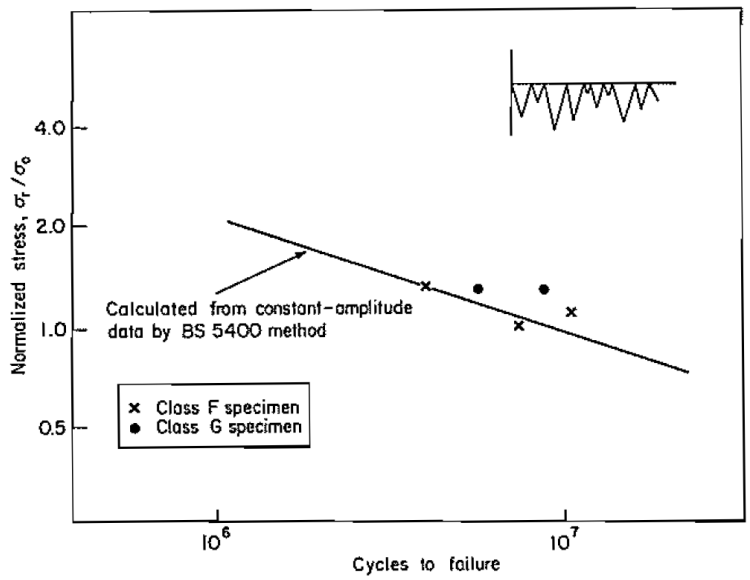

Figure 6: Variable amplitude performance for pulsating compression in [5]

Gurney (1985) [6] carried out fatigue tests using specimens made from BS4360 Grade 50 Steel, as shown in Figure 7, under both constant and variable amplitude axial loading. Both as-welded and stress relieved specimens were tested.

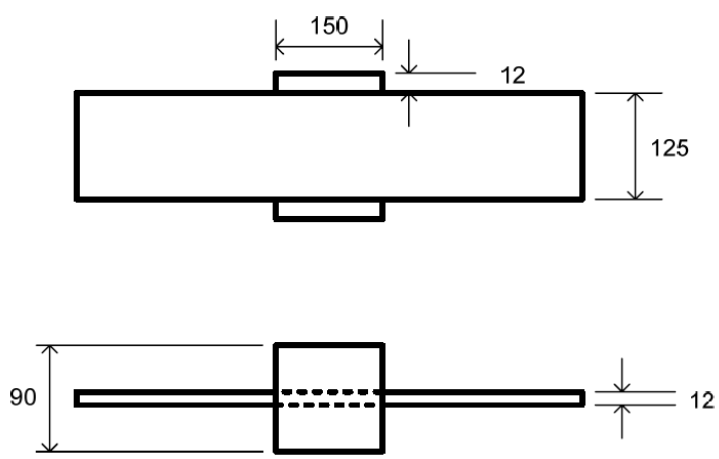

Figure 7: Specimens tested in [6,8-9]

The constant amplitude loading tests were carried out with stress ratios of $R = 0$ and $R = -1$, while the variable amplitude loading tests were carried out using various short sequences and under a Raleigh spectrum. The constant amplitude fatigue tests results for as welded specimens with S-N curves fitted with inverse slope of 3 are given in Figure 8. Stress relief had virtually no effect on fatigue strength at $R = 0$ but improved strength by about 25% at $R = -1$. The results suggested that for $R = 0$, as-welded or stress-relieved, and for $R = -1$ as-welded, the whole of the stress range was damaging. But for $R = -1$,

stress-relieved, it appeared that only about 50% of the compressive part of the range was damaging.

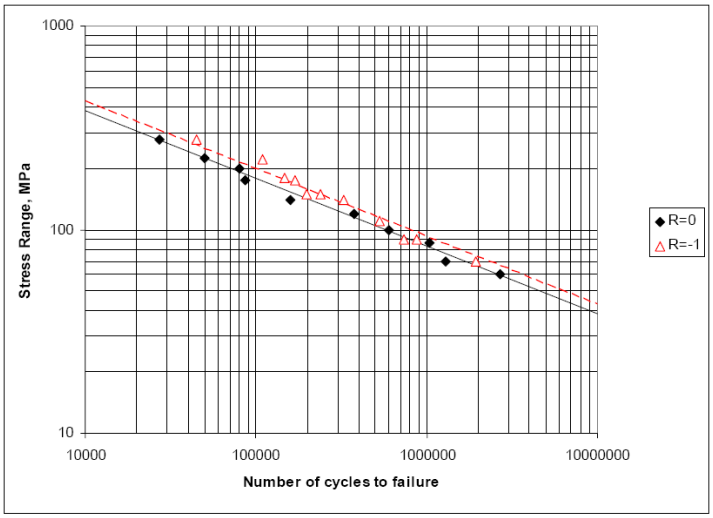

Figure 8: Constant amplitude fatigue tests results in [6]

Niemi (1987) [7] conducted two series of fatigue tests, one on butt welded specimens and another on fillet welded knee joints under both constant and variable amplitude loading. The variable amplitude loading was generated using the Markow's matrix technique. The material used was high tensile steel HSF 490 (yield stress of 492-496 MPa) in 5 and 8 mm thickness. The stress ratio varied between 0.01 and 0.75 and between -0.13 and 0.42 (for maximum stress in the cycle) for butt welded joints tested under constant amplitude and variable amplitude loading, respectively. The stress ratio varied between 0.56 and 0.84 and between 0 and 0.55 (for maximum stress in the cycle) for fillet welded knee joints tested under constant amplitude and variable amplitude loading, respectively. No significant difference was found for constant and variable amplitude test results in terms of equivalent stress in the latter. Also there was no difference between fatigue test results for various stress ratios, possibly since all the mean stresses were tensile.

Gurney (1988) [8] carried out fatigue tests on longitudinal non-load-carrying fillet welded edge attachments, as shown in Figure 7, under two basic spectra based upon the two parameter Weibull distribution, as shown in Figure 9. The influence of stress ratio varied markedly with the form of the loading spectrum. Under wide band loading (variable mean stress) the fatigue life under spectra having the peak range at R = -1 was typically 30% greater than when the peak range was at R = 0. However, with all cycles at R = -1, the life was 17-57% less than when all cycles were at R = 0. Similarly under programme loading the lives at R = -1 were again less than at R = 0.

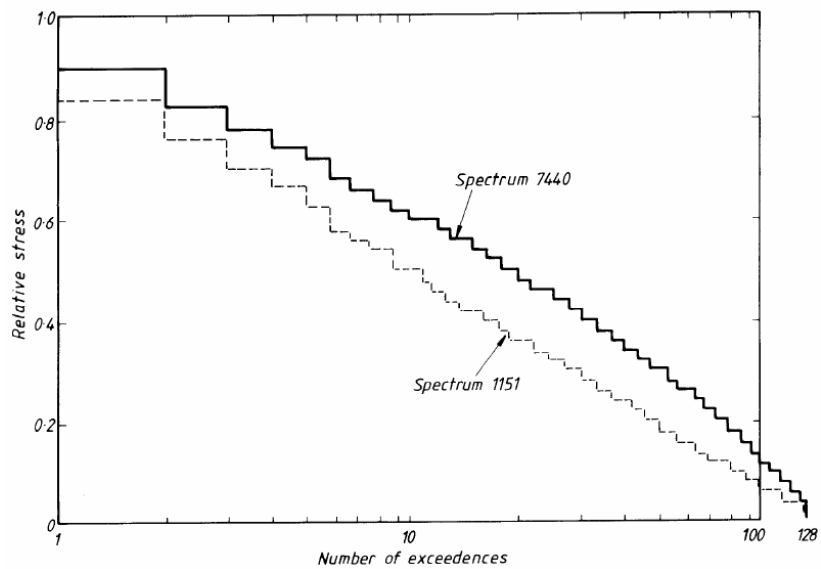

Figure 9: Two basic spectra based upon the two parameter Weibull distribuion in [8]

Gurney (1992) [9] performed fatigue tests on as-welded and stress relieved joints made from high tensile steel under both constant and variable amplitude axial loading. The variable amplitude spectrum was based upon the two parameter Weibull distribution, as shown in Figure 9. Specimen dimensions are shown Figure 7. The steel used was BS 4360-50D with a yield stress of 347-385 MPa and RQT 700 with a yield stress of 805 MPa.

Under constant amplitude pulsating tension (R = 0), as-welded and stress relieved specimens had identical fatigue strengths. Under alternating (R = -1) loading, there was a significant difference in fatigue strength between the as-welded and stress relieved specimens. The fatigue enhancement factor was 1.41. For the RQT 700 specimens, rather surprisingly the results at R = 0 are slightly higher than the corresponding results for Grade 50 material; in fact the two results obtained at R = 0.5 lie almost exactly on the S-N curve for Grade 50 at R = 0. The three specimens tested at higher stress ratios showed a distinct reduction in strength.

Under variable amplitude loading, with the main stress cycle at R = 0 there was no noticeable difference between the fatigue lives for as-welded and stress relieved joints. With the main stress cycle at R = -1, stress relief gave a substantial increase in life (by a factor of more than 2). This mirrors the corresponding increase in life that also occurs under constant amplitude loading. Tests on as-welded joints of high tensile steel under 'stalactitic' loading (with all stresses pulsating downwards from a peak stress of 500 MPa) led to a decrease in life by a factor of 5 compared with the life of specimens subjected to the same spectrum at R = 0. The Miner's rule gave unconservative prediction for the majority of the specimens, both as-welded and stress relieved, tested under wide band loading, both at R = 0 and at R = -1, and under stalactitic loading.

Rörup and Petershagen (2000) [10] and Rörup and Fricke (2004) [11] tested longitudinal stiffeners with non-load carrying fillet welds, as shown in Figure 10, under constant

amplitude and variable amplitude axial loading. The specimens were made of structural steel S355 J2 G3, with 355 MPa minimum yield strength.

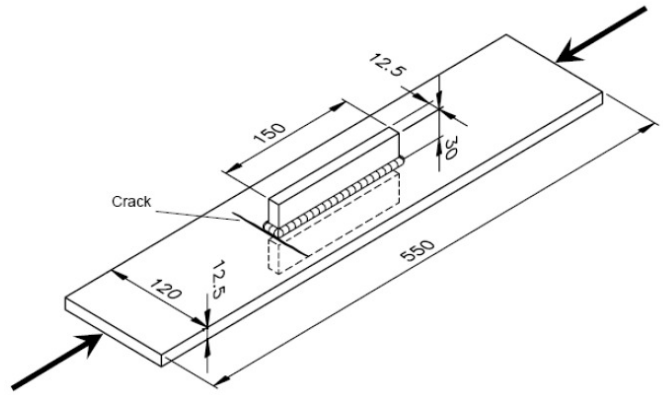

Figure 10: Fatigue test specimen in [10-11]

The constant amplitude loading tests were performed with the stress ratios shown in Figure 11. The fatigue test results for $R = -\infty$ are shown in Figure 12, which also includes the fitted S-N curve for various probabilities of survival (Ps). The fatigue enhancement factor for fully compressive cycles was 1.46 as compared with fully tensile cycles. With a constant crack initiation life for different stress ratios, the increase in total fatigue life under fully compressive constant amplitude loading is caused by the crack propagation phase.

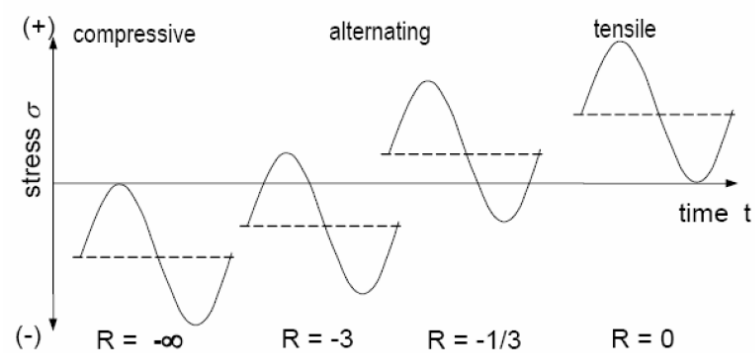

Figure 11: Applied stress ratio in [11]

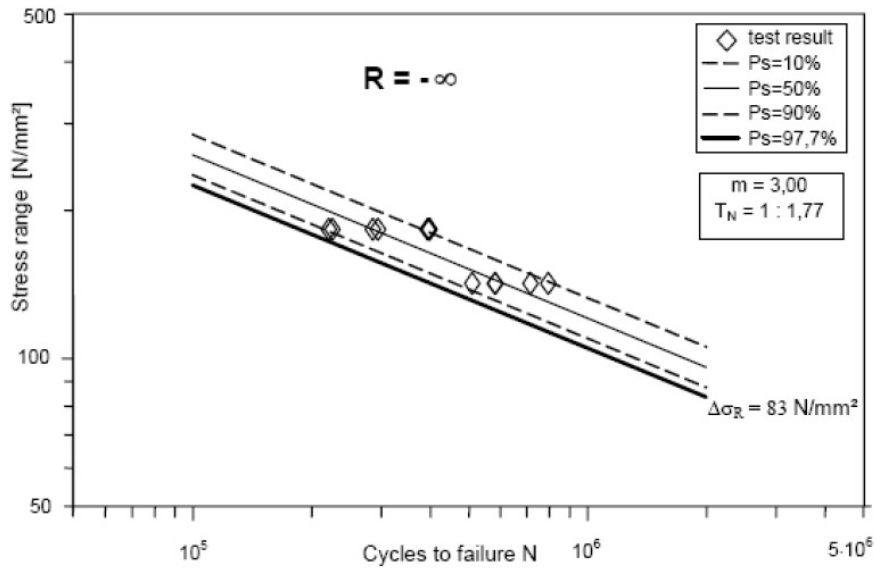

Figure 12: Fatigue tests results and fitted S-N curves for *R* = -∞ in [11]

The random load sequence applied in [10] was log-linear distributed, corresponding to the a long-term distribution of sea-way loads for ships. The load spectra are provided in Figure 13. Due to residual tensile stresses, the crack initiation life was independent of the stress ratio, but during the crack propagation phase, there were significant effects in case of compressive mean stresses. It was concluded that the permissible nominal stress for the investigated specimen under cyclic compressive loading could be at least up to 35% higher than under cyclic tensile loading. Figure 14 presents the effect of stress ratio on the fatigue enhancement factors for fatigue strength for both the constant and variable amplitude loading applied in [10-11].

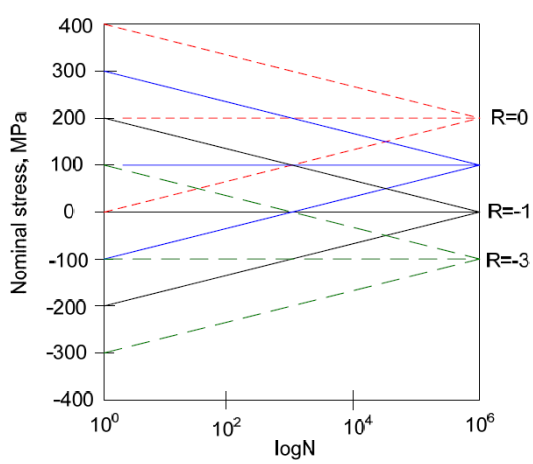

Figure 13: Load Spectra for tests under random loading in [10]

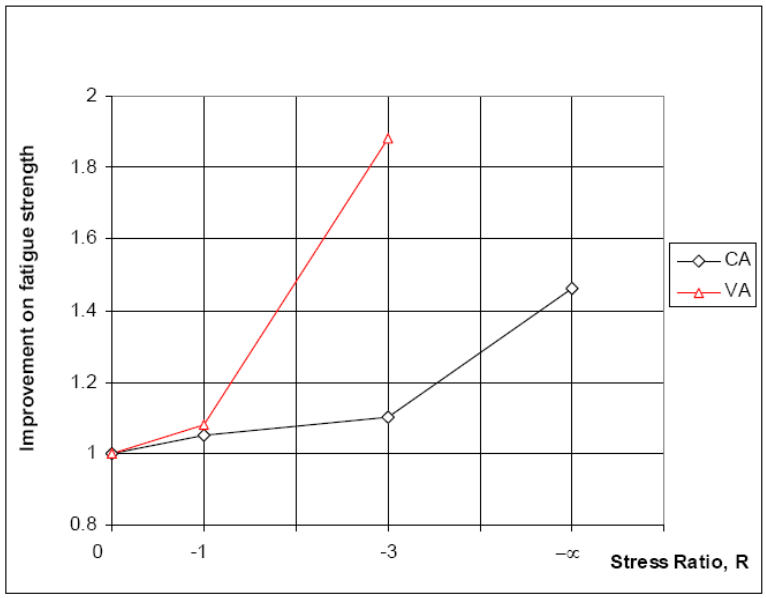

Figure 14: Improvement factors on fatigue strength for constant and variable amplitude loading in [10-11]

Marquis and Mikkola (2001) [12] performed fatigue tests under load controlled three point bending on I-beam type structures made from high strength steel (HTS390) in an as-welded condition using constant amplitude loading and two spectra considered as representative for ships. The specimen dimensions are given in Figure 15. The results showed that the mean fatigue life for the block wise changing mean stress spectrum was 2.2 times greater than for the constant tensile mean stress spectrum, although the maximum stress range was greater for the former spectrum. This confirmed the non-damaging effect of the compressive part of the cycle.

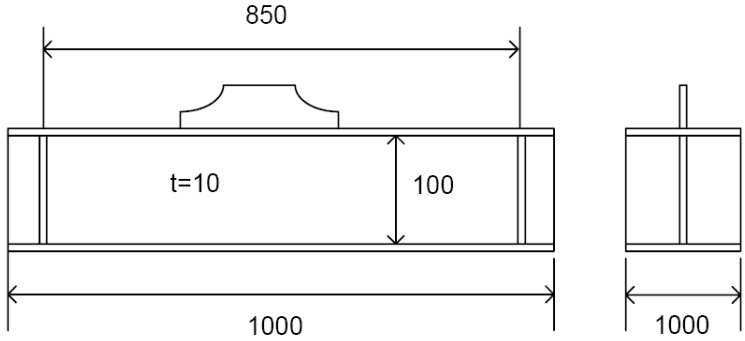

Figure 15: Specimen dimensions in [12]

Sonsino, Maddox and Hobbacher (2003) [13] investigated the cumulative fatigue damage carried out on two types of welded joints (butt welds and transverse stiffeners, shown in Figure 16), made of S335M, S690Q and S960Q structural steel, using a modified Palmgren-Miner linear cumulative damage rule. The tests were carried out under both constant and variable amplitude loading, with fully reversed (R = -1) and pulsating (R = 0) cycle. For the variable amplitude loading, both a base Gaussian spectrum and one in which a Gaussian overload spectrum was superimposed onto the normal Gaussian

spectrum were applied, with an irregularity factor of I = 0.99, as shown in Figure 17. The results showed that fatigue had not depended on the steel type, but only on the loading mode. The mean stress did not influence the fatigue life, probably because of existing high tensile residual stresses. For variable amplitude loading, the actual fatigue life lay between 1/3 and 3 times the fatigue life predicted by the modified Palmgren-Miner linear cumulative damage rule.

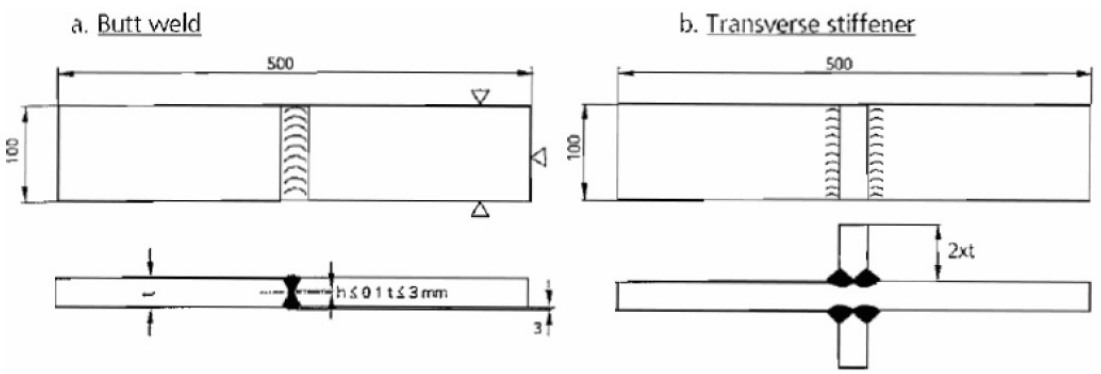

Figure 16: Dimensions of the welded specimens in [13]

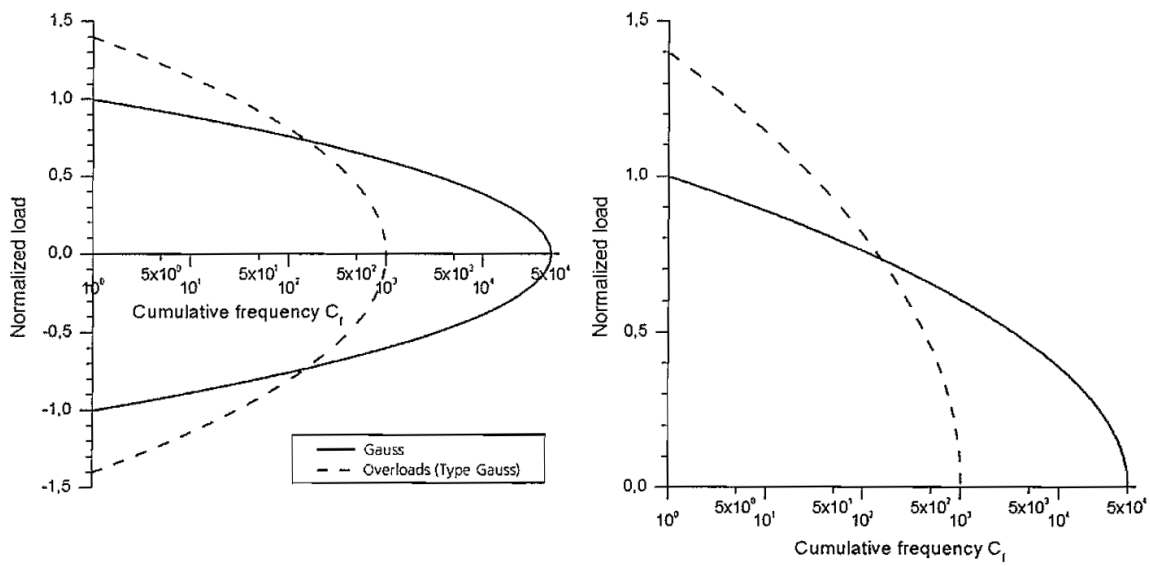

Figure 17: Gaussian load spectrum with overloads applied in [13]

Kassner and Krebs (2007) [14] investigated the relation between the notch effect and the mean stress effect on the fatigue strength of welded components. Experimental results of small scale specimen tests showed a decreasing effect of mean stress as a consequence of increasing notch effect. In fact, the fatigue strength of a welded joint with very high notch effect can be independent of mean stress. In Figure 18, the enhancement factor f(R), which describes the influence of the mean stress on the fatigue strength, is represented as dependent on the notch effect for different welded joint types. As seen from Figure 18, the effect of mean stress is insignificant for welded joints with high stress concentration typical for ship structures.

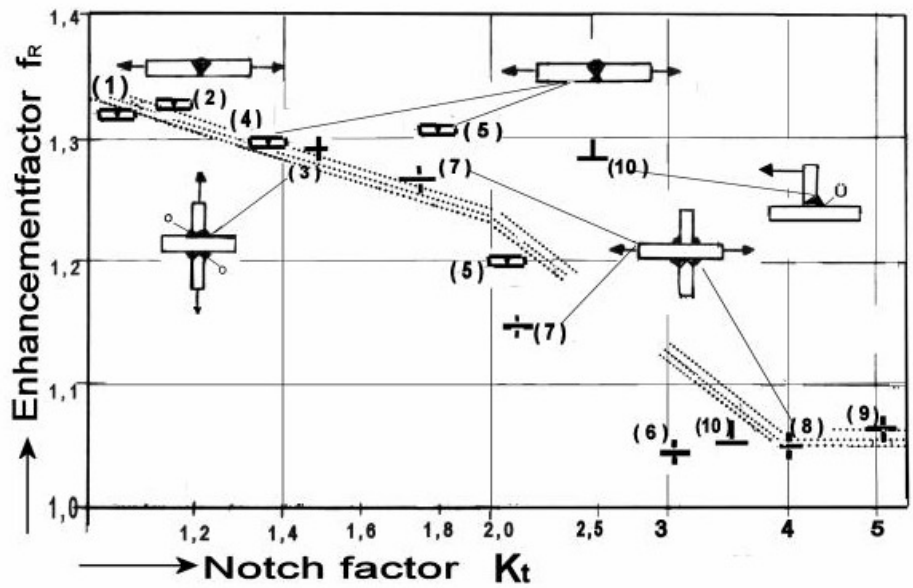

Figure 18: Example of the influence of the notch effect on the mean stress dependence in different welded joints after [14]

(1) Butt weld, 10x50 mm², S690, GTA;
(2) Butt weld, 20x50 mm², SM490;
(3) Cruciform joint, K-butt weld, grinding, S355;
(4) Butt weld, 12 x 100 mm², S355, GMA;
(5) Butt weld, 10 x 100 mm², S355M, GMA;
(6) Butt weld, 30 x 100 mm, S355, GMA;
(7) Transverse stiffener, 12x40 mm², fillet weld, S355;
(8) Transverse stiffener, 10x100 mm², K-butt weld; S355;
(9) Transverse stiffener 30 x 100 mm², K-butt weld, MAG
(10) T-joint, 15 mm/40 mm, S355

Hobbacher (2007) [15] provided the following guidance to account for the effect of stress ratio (or mean stress effect), as shown in Table 1. If no reliable information on residual stress is available, an enhancement factor f(R) = 1 is recommended. Other factors should only be used if reliable information or estimations of the residual stress level are present.

Table 1: Recommendations for fatigue enhancement factors in [15]

Cases	Fatigue Enhancement Factor (f(R))
Unwelded base material and wrought products with negligible residual stresses. Stress relieved welded components.	f(R) = 1.6 for $R < -1$ f(R) = -0.4R + 1.2 for $-1 \leq R \leq 0.5$ f(R) = 1 for $R > 0.5$
Small scale thin-walled simple structural elements containing short welds. Parts or components containing thermally cut edges.	f(R) = 1.3 for $R < -1$ f(R) = -0.4R + 0.9 for $-1 \leq R \leq -0.25$ f(R) = 1 for $R > -0.25$
Complex two- or three-dimensional welded components. Components with global residual stresses. Thick-	f(R) = 1 (no enhancement)

walled components. Normal case for welded components and structures.	

Heo et al (2007) [16] tested transverse fillet welded specimens, shown in Figure 19, under seven strain controlled programs to investigate the effect of tensile and compressive static stress in ship structures. The specimens were made from A Grade steel. The load cases consisted of various combinations of high (HCF) and low (LCF) cycle fatigue loading. Load cases 1 to 3 are shown in Figure 20. The results showed that HCF cyclic loading with compressive mean stress does not contribute to fatigue damage. Tensile mean stress induced an increase in fatigue damage, and compressive mean stress had the opposite effect.

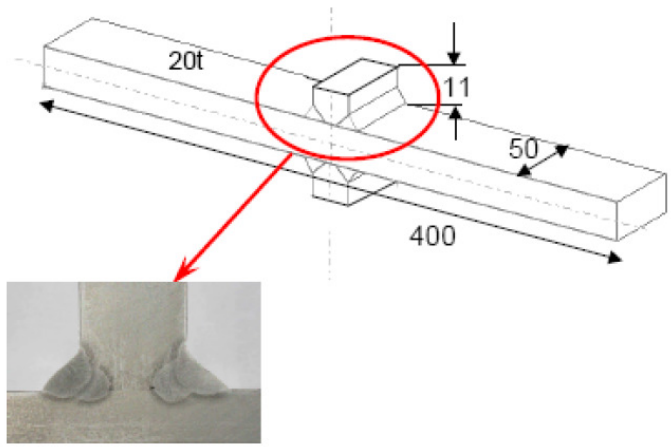

Figure 19: Geometry of welded cruciform joint in [16]

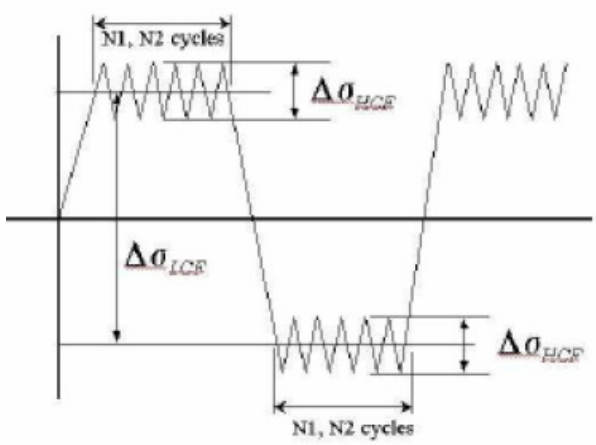

Figure 20: Load cases 1 to 3 for combined fatigue damage test in [16]

Bousseau and Millot (2008) [17] carried out fatigue tests under pulsating compression on test specimens made from 100 HLES steel with T-shaped welded joints and/or longitudinal attachments made from S355 NL steel. The tests demonstrated that initiation can occur at high loading levels; however propagation remains limited and did not exceed the plastic zone dimensions.

Gadouini et al (2008) [18] introduced artificial spherical defects at the surface of fatigue samples made in C 35 steel and conducted tension and torsion fatigue tests in order to determine the fatigue limit. The results showed that under tension, a positive mean stress lowered the fatigue limit and vice versa. Under torsion, the mean stress did not influence the fatigue limit when the value was lower than the yield stress of the material, as shown in Figure 21. This result was similar to the behaviour of defect free materials. In addition, several models were used to describe the influence of mean stress on the fatigue limit. It was concluded that the local stress state should be considered at the tip of the defect and the nonlinear kinematic hardening was necessary to describe local stress relaxation when $R \neq 0$.

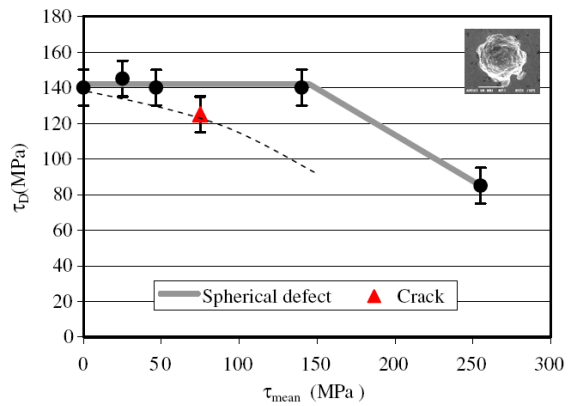

Figure 21: Evolution of the fatigue limit versus mean stress under torsion loading in [18]

Polezhayeva (2010) [2] performed fatigue testing on both longitudinal fillet welded plate specimens (Figure 22) and welded panels (Figure 23) representing a typical longitudinal stiffener to transverse web connection in a ship's hull. The specimens and panels were manufactured from Lloyd's Grade A steel plates with a specified minimum yield strength of 235 MPa. The plate specimens were tested in both as-welded and stress relieved conditions, while the panels were tested in as-welded conditions only. Both constant and variable amplitude loading tests were conducted. The constant amplitude loading consisted of fully tensile (R = 0.1), fully compressive (R = -∞) and alternating cycles (R = -1), while the variable amplitude loading applied was based upon the Rayleigh distribution close to those experienced in ships.

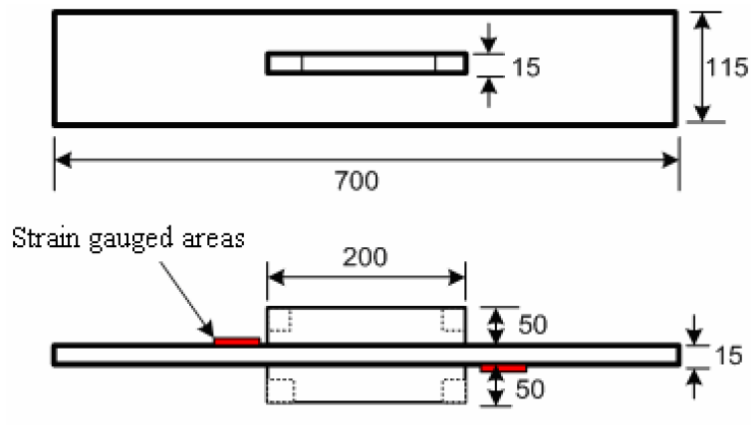

Figure 22: Plate specimen design in [2]

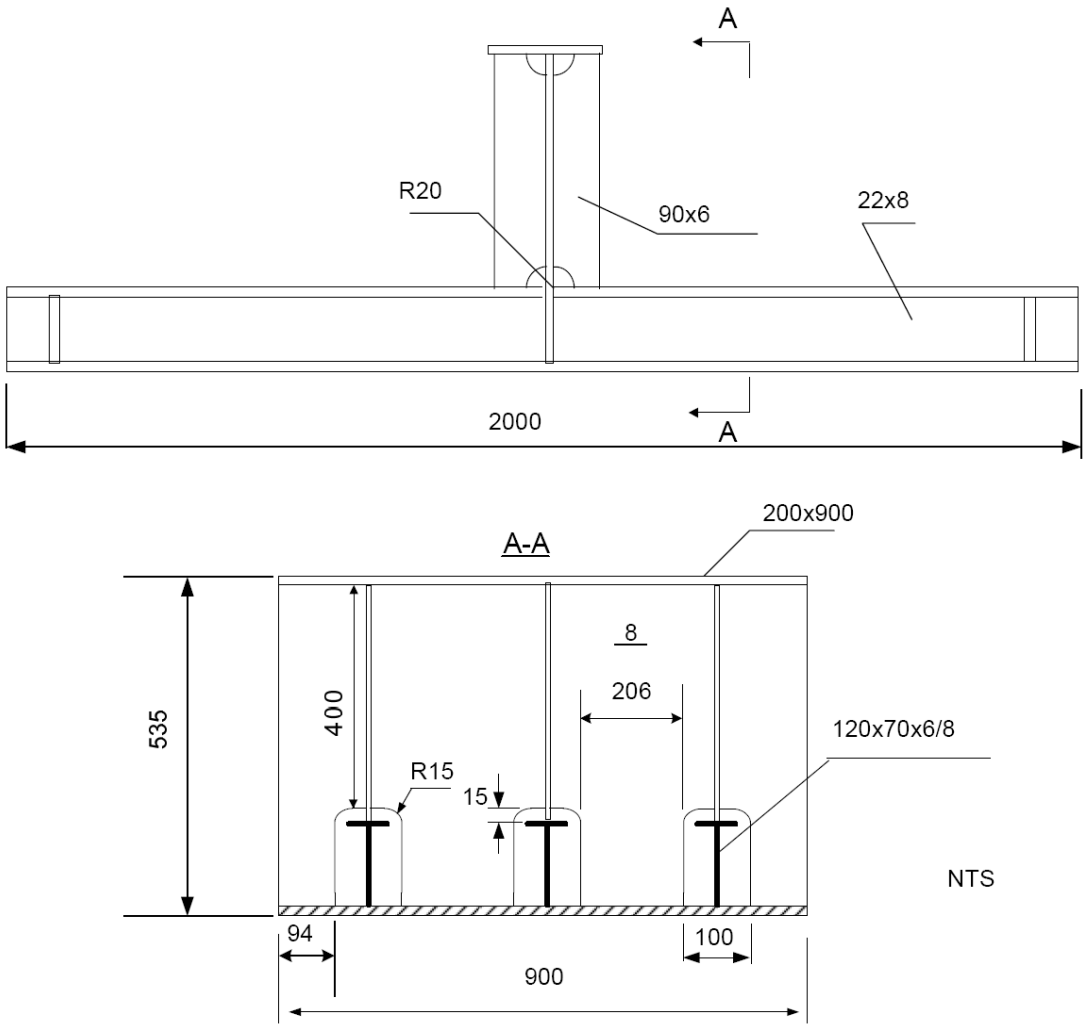

Figure 23: Reduced scale welded panel design in [2]

The constant and variable amplitude tests results for the plate specimens are shown in Figure 24 and Figure 25, respectively. Under constant amplitude loading, for as-welded

specimens, there was very little scatter between the different modes of loading, likely due to the influence of the tensile residual stresses at the weld toe. Heat treated specimens showed fatigue behaviour directly affected by the applied mean stress. Stress-relief was beneficial, but only if the applied loading was partly or fully compressive. Stress-relieved welded joints were unlikely to suffer significant fatigue damage if they experienced only compressive applied stresses. The results from stress-relieved specimens tested with $R = 0.1$ were seen to be essentially the same as those obtained from the as-welded specimens. Under variable amplitude loading, specimens under fully compressive load showed a better fatigue life. Apart from some of the results for fully compressive loading, all the results agreed with the constant amplitude loading, which would indicate that Miner's rule was accurate for the plate specimens and the loading spectra investigated.

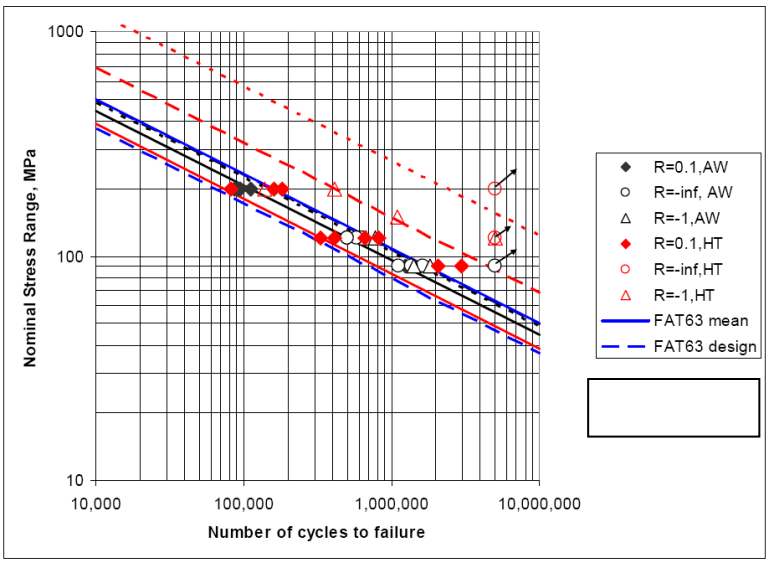

Figure 24: Constant amplitude fatigue tests results of the plate specimens in [2]

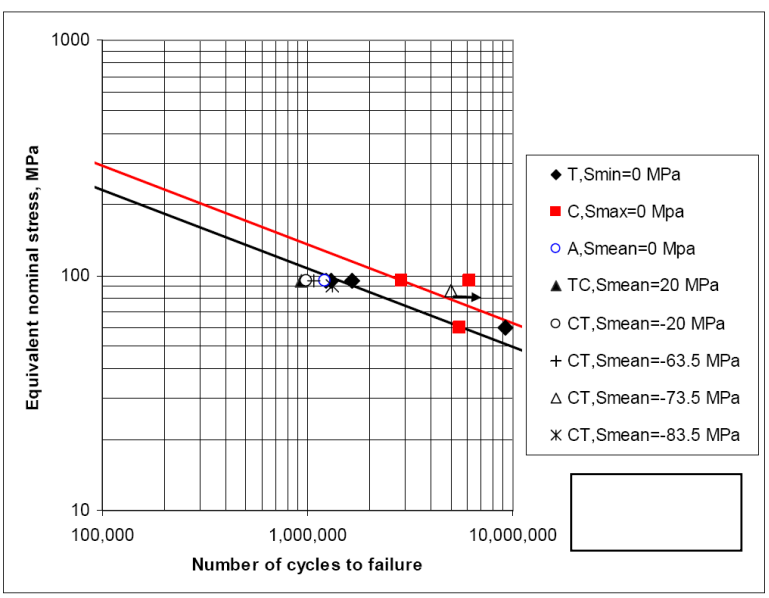

Figure 25: Variable amplitude fatigue tests results of the plate specimens in [2]

The fatigue test results for the welded panels are shown in Figure 26. The welded panels showed a similar trend to the plate specimens under variable amplitude, i.e. the mean stress has no effects except when the cycle was fully compressive. Under variable amplitude loading, the test under predominantly compressive stresses gave a life about 50% longer than the test under predominantly tensile stresses. The residual stress relaxation due to the applied fatigue loading was beneficial if the subsequent fatigue loading produced effective stress ranges that were partly compressive.

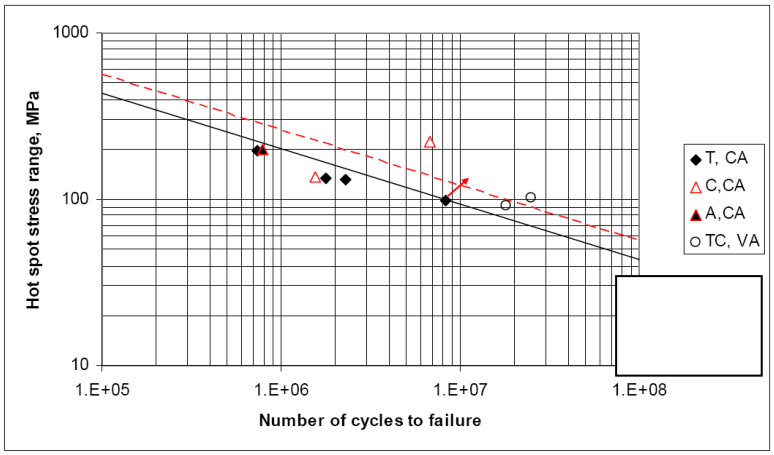

Figure 26: Fatigue test results of the welded panels in [2]

Colin et al (2010) [19] conducted fatigue tests on cylindrical solid specimens made from Aluminum 7075-T6 and stainless steel 304L under both strain control and load control constant amplitude loading. The specimen geometry for stainless steel 304L is shown in Figure 27. Effects of loading sequence, mean strain or stress, and prestraining were investigated. The behaviour of aluminum was shown not to be affected by preloading, whereas the behaviour of stainless steel is greatly influenced by prior loading. A fatigue life parameter with both stress and strain terms was necessary to correlate the stainless steel data with deformation history effects. The Smith-Watson-Topper parameter [20] was shown to correlate most of the data reasonably well for both the stainless steel and aluminum, as shown in Figure 28.

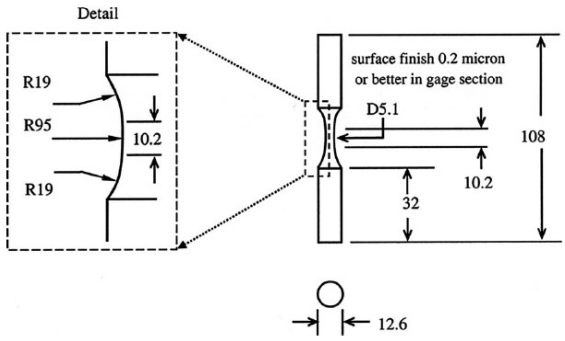

Figure 27: Specimen geometry for stainless steel 304L in [19]

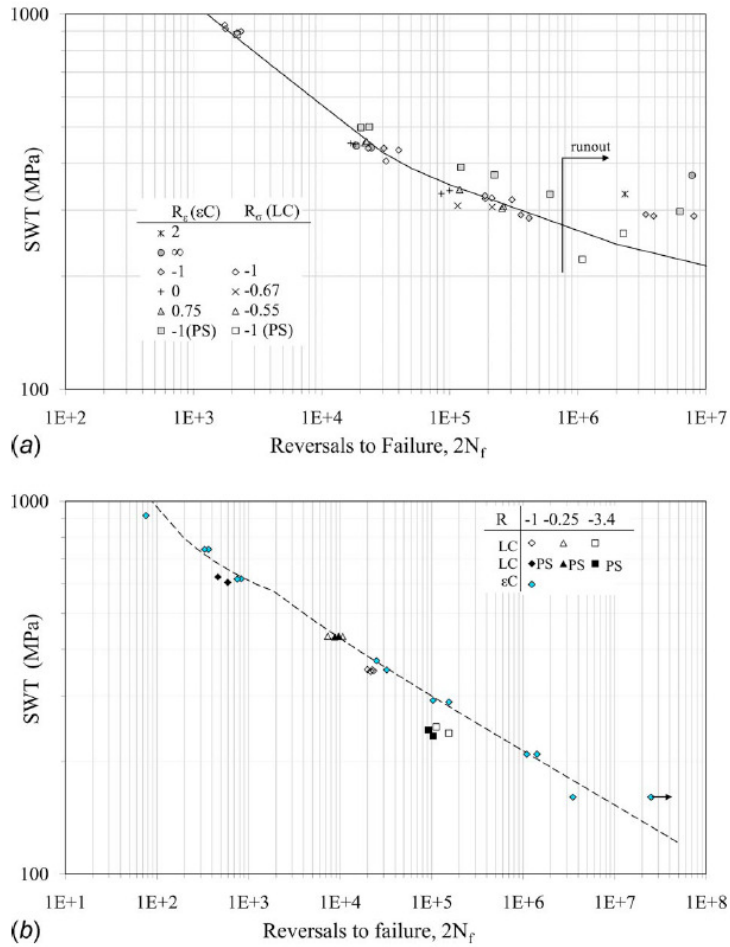

Figure 28: SWT versus reversal to failure for: (a) stainless steel 304 and (b) aluminium 7075-T6 in [19]

Aid et al (2011) [21] carried out fatigue tests under block loading and random loading on tensile specimens made from aluminum alloy 6082 T 6. They also proposed a "damaged stress interaction damage rule" to take into account the damage evolution at different load levels and allow the effect of the loading sequence to be included. The results showed that the proposed model allowed a better fatigue damage prediction than the widely used Palmgren-Miner rule.

Based on the literature review in this section, the following conclusions can be drawn:

The mean stress effect is a function of the notch factor of the welded joint. There is a decreasing effect of mean stress as a consequence of increasing the notch effect. In fact, the fatigue strength of a welded joint with very high notch effect can be independent of mean stress.

The compressive part of a fatigue cycle is only partly damaging, but down to a stress ratio of $R = -1$, the compressive part has no significant benefit on the fatigue strength. This applies to the welded joints with severe stress concentrations and the presence of

high residual stresses, typical of ship details under constant and variable amplitude fatigue tests .

On the other hand, enhancement of the fatigue strength was observed under fully compressive applied stress ranges ($R = -\infty$). Under fully compressive applied ranges, the enhancement factor on fatigue strength (f(R)) varied widely from 1.17 to 1.48.

There is not much data on the benefit of partly compressive cycles where the compressive part of the cycle is larger than the tensile part (i.e. stress ratios between $R = -1$ and $R = -\infty$). However, there is an indication that there is an influence of mean stress under ship related variable amplitude loading.

2.3 EFFECT OF MEAN STRESS ON FATIGUE STRENGTH OF SMALL SPECIMENS AND COMPONENTS WHEN OVERLOAD IS APPLIED BEFORE FATIGUE TESTS

Static loading on a ship structure induced either by water pressure before service, such as a tank test and ballasting, or by static cargo or ballast pressure during laden or ballast voyages, can cause relatively high static mean hot spot stresses at welded joints, compared with cyclic loadings induced by waves during service. Due to these static pre-loadings, the initial tensile residual stresses at welded joints and/or flame cut edges, where fatigue strength is of concern(in most cases, where stress concentration occurs), are expected to be shaken-down to a great extent by the elasto-plastic deformation behaviour of the material. However, not every fatigue prone welded joint in ship is subjected to tank test and ballasting static loading, so residual stress relaxation due to these loads is not guaranteed. On the other hand, static loads due to cargo or ballast pressure are unavoidable. Ship structural members are then exposed to cyclic loading during their service. The effects of such shake-down on the mean stress effect on the fatigue strength were reviewed in this section.

Hyundai Heavy Industries (2000) [22] investigated the effects of the mean stress on the fatigue strength of preloaded specimens. Various types of specimens made from grade "A" mild steel and grade AH32 high tensile steel were tested, as shown in Figure 29. Table 2 shows the types of static pre-loads and mean stresses applied to the specimens.

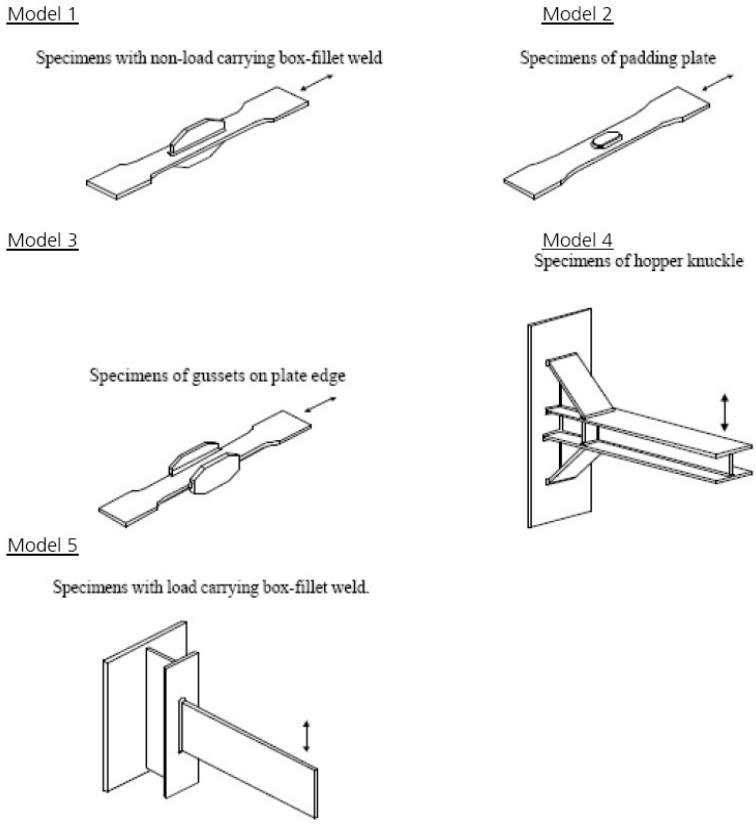

Figure 29: Details of specimens in [22]

Table 2: Types of static pre-loads and mean stresses applied in [22]

Condition	Model 1, 2 & 3	Model 4 & 5
1	Pre-load = 0 Mean stress = 0 	Pre-load = 0 Mean stress = 0
2	Pre-load = 0.5 σ_0 Mean stress = 0 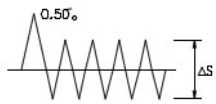	Pre-load = 0.5 σ_0 Mean stress = 0 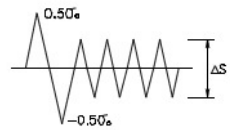
3	Pre-load = 0.85 σ_0 Mean stress = 0 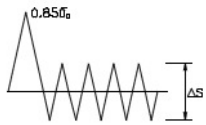	Pre-load = 0.85 σ_0 Mean stress = 0 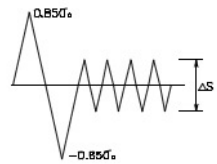
4	Pre-load = 0.85 σ_0 Mean stress = 0.5 σ_0 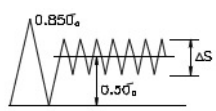	Pre-load = 0.85 σ_0 Mean stress = 0.5 σ_0 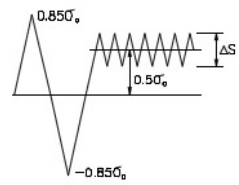
5	Pre-load = 0.85 σ_0 Mean stress = 0.85 σ_0 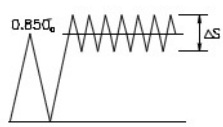	Pre-load = 0.85 σ_0 Mean stress = 0.85 σ_0 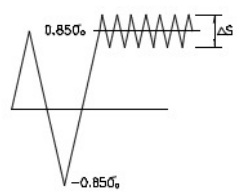

σ_0 = yield stress (σ_y)

Figure 30 shows some typical fatigue tests results in [22]. The results showed that for a hot spot preload above yield (σ_y), the fatigue strength decreased with an increase in the hot spot mean stress of the fatigue cycles, such that the fatigue strength ratio varied between 0.6-0.8 if the hot spot mean stress was between 0.5-1.5 σ_y and below 0.6 if the hot spot mean stress was above 1.5 σ_y. Here, the fatigue strength ratio was calculated with respect to fatigue strength obtained for alternating tests (zero mean stress). The fatigue strength for alternating cycle tests increased almost linearly with increase in pre-load, if the hot spot pre-load was above 0.6 σ_y, with the strength ratio reaching 1.4 for 1.6 σ_y. Here, the fatigue strength ratio was calculated with respect to fatigue strength obtained for alternating tests with no preload. This confirmed the occurrence of relaxation of residual stress if a large initial stress was applied. The results suggest that if the initial hot spot preload was below 0.6 σ_y, there was no significant relaxation of the residual stress. Although the results of the tests showed significant influence of initial

preload (or overload), the influence of the preload on largely or fully compressive fatigue cycles was not investigated.

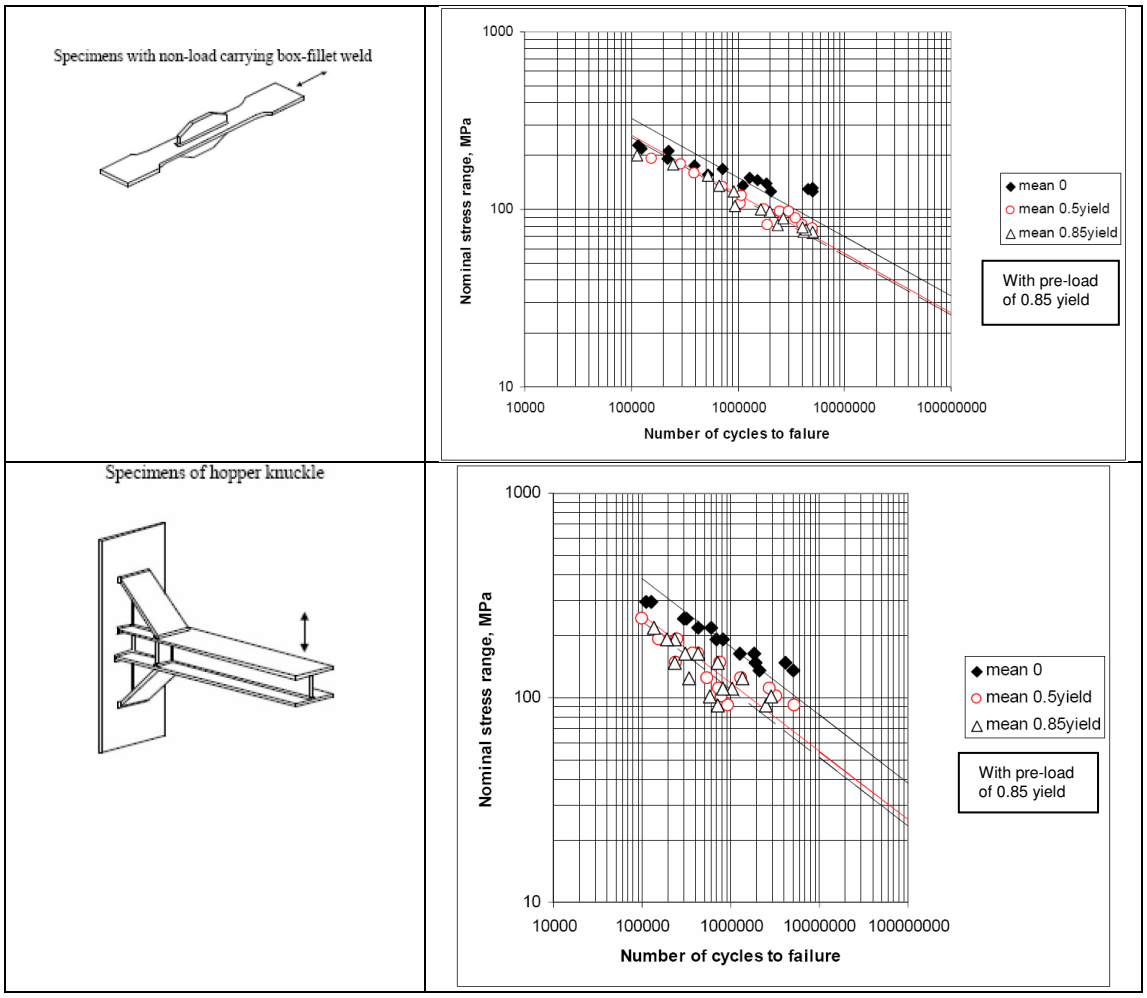

Figure 30: Typical fatigue test results in [22]

Lotsberg and Landet (2004) [23] tested two full scale models of a side longitudinal, as shown in Figure 31, made from NVD36 steel under constant amplitude four-point bending. Two fatigue load conditions were considered: ballast (tension at the hot spot, R = 0.16) and loaded (compression at the hot spot, $R = -\infty$). Before the start of fatigue testing, the specimens were exposed to the load cycles representing the testing of ballast tanks and the maximum load amplitudes from a 1-year storm. The fatigue life was 819,777 cycles for the ballast condition and 6,600,000 cycles for the loaded conditions, which represented an enhancement factor of around 2 on fatigue strength.

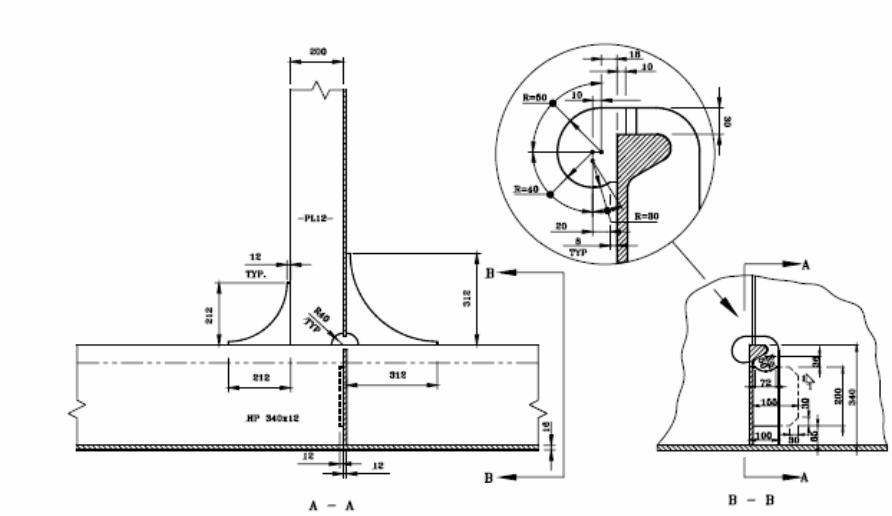

Figure 31: Full scale models of side longitudinal tested under four-point bending in [23]

2.4 MEASUREMENTS OF RELAXATION OF WELDING RESIDUAL STRESS

Borgren and Lopez Martinez (1993) [24] reported spectrum fatigue testing and residual stress measurements on non-load carrying fillet welded test specimens, similar to those used by Maddox [25]. It was found that the residual stresses in the as-welded condition were close to the yield stress of the material. These residual stresses were found to relax very rapidly; within 8% of the total specimen life, 50% or more of the initial stresses were relaxed.

Nitschke-Pagel (1994) [26] measured the relaxation of residual stress under fatigue load for a transverse load-carrying butt weld (small-scale specimen) made from S690 steel. The measurements are shown in Figure 32. Transverse residual stresses were reduced almost completely after 10^5 load cycles. This was also true for longitudinal residual stresses in weld toe.

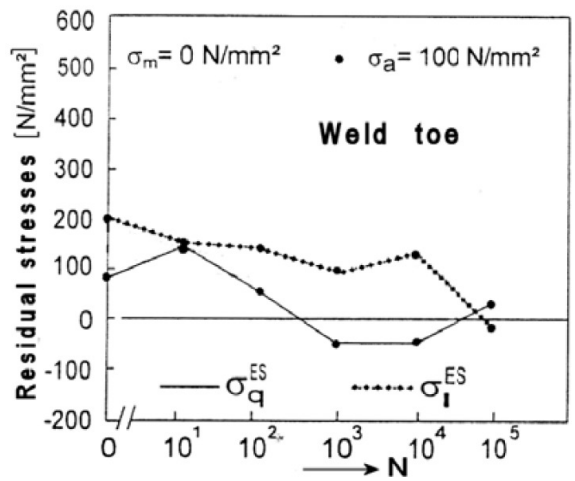

Figure 32: Variation of residual stresses in the butt weld of S690 specimen in [26]

Blom (1995) [27] reported experiments in which residual stress measurements were performed before cycling and at two different numbers of fatigue cycles, neither of which was a single cycle. He found some appreciable relaxation between the two cycle counts in some tests, although the largest relaxation (50 to 80% of the initial value) was recorded at the first cycle count.

Lopez Martinez et al (1997) [28] published maps of residual stress distributions measured by neutron diffraction for as-welded and TIG-dressed specimens with and without static loading or spectrum fatigue cycling. They concluded that the static load caused appreciable relaxation and that the variable amplitude fatigue loading showed the same degree of relaxation as the static load case, suggesting that the fatigue relaxation occurred early during the fatigue loading and was correlated to the occurrence of maximum load in the spectrum.

Numerous researchers have reported significant relaxation and redistribution of residual stresses on the first loading cycle, followed by minimal further relaxation on subsequent cycles. Iida et al (1997) [29] and Iida and Takanashi (1998) [30] reported this result for both $R = 0$ and $R = -1$ cycling of notched specimens. Typical results for the change in the residual stress at a single point near the weld centre line with cycling are shown in Figure 33. It should be noted that the magnitude of the decrease in the residual stress on the first cycle corresponds with the magnitude of the applied static stress, indicating a simple shakedown behaviour.

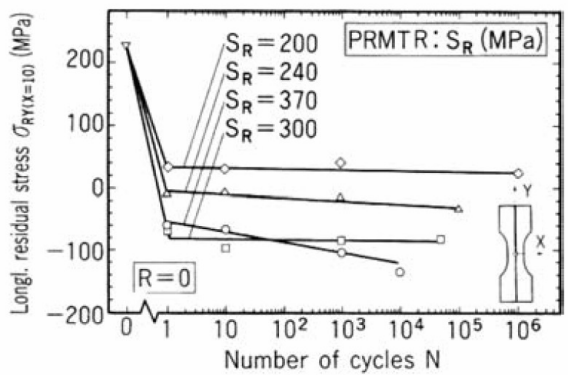

Figure 33: Change in longitudinal residual stress at a distance of 10 mm from the weld centre line with application of static or fatigue loads in [30]

Takanashi et al (2000) [31] found a similar result for smooth butt welds and proposed a simple mechanics model as an explanation. Typical changes in the residual stress profile after fatigue cycling at two different stress amplitudes are shown in Figure 34. It should be noted that both the tensile and compressive residual stresses are relaxed towards zero, although the changes are more pronounced for the tensile stresses.

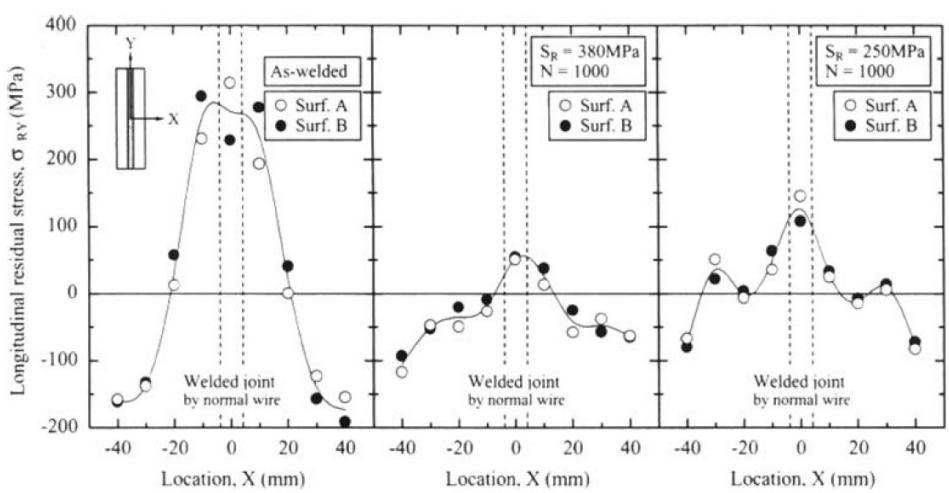

Figure 34: Change in longitudinal residual stress at a distance of 10 mm from the weld centre line with application of static or fatigue loads in [31]

Hyundai Heavy Industries (2000) [22] measured the initial residual stress and residual stress distribution after application of static loads with a magnitude of 0.5 σ_y and 0.8 σ_y in the specimens shown in Figure 29. Numerical simulations of the residual stress

redistribution were also performed. Typical measured and calculated residual stresses before and after the application of static loads are presented in Figure 35 and Figure 36.

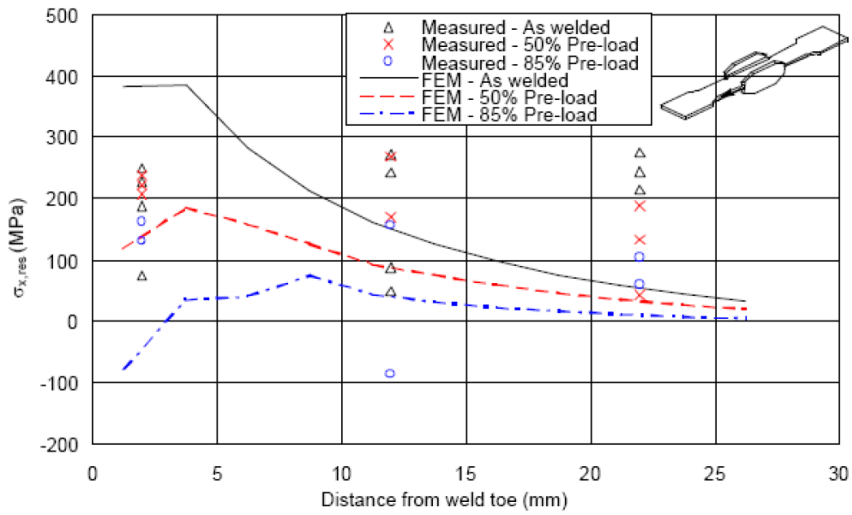

Figure 35: Residual stress distribution at the edge of the main plate (Model 2) in [22]

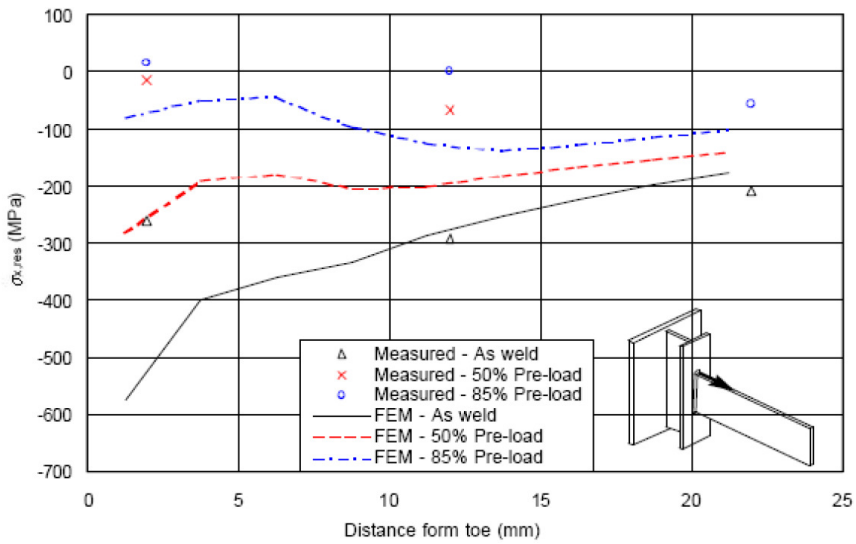

Figure 36: Residual stress distribution at the edge on the upper part (Model 5) in [22]

Nitschke-Pagel and Wohlfahrt (2000) [32] measured a relaxation of residual stresses in welded high strength steel in proportion to the magnitude of a single applied static tensile load, but observed minimal changes with further cycling, and minimal changes with static compressive loads.

Lachmann et al (2000) [33] confirmed the same general trends with corresponding Barkhausen Noise measurements of residual stress.

Han and Shin (2002) [34] found a large change in residual stresses on the first load cycle for low strength steel, but very small changes with further cycling.

Dattoma et al (2004) [35] developed a finite element model of residual stress relaxation in weldments that predicted significant changes on the first cycle but no further changes after 10 cycles.

Barsoum and Gustafsson (2007) [36] carried out constant and variable amplitude fatigue testing on out-of plane gusset fillet welded high strength steel joints, in order to study the influence of the residual stress on the fatigue strength. Residual stress measurements were carried out close to the weld toe in order to study the relaxation due to variable amplitude fatigue. The base material used to fabricate the welded joints was a cold formed high strength steel, Domex 700 MC, with a minimum yield strength of 700 MPa and a minimum tensile strength of 750 MPa. The weld fillers used were OK Autrod 12.51 (Conventional) and OK Tubrod 15.55 (LTT). Figure 37 illustrates the welded specimens.

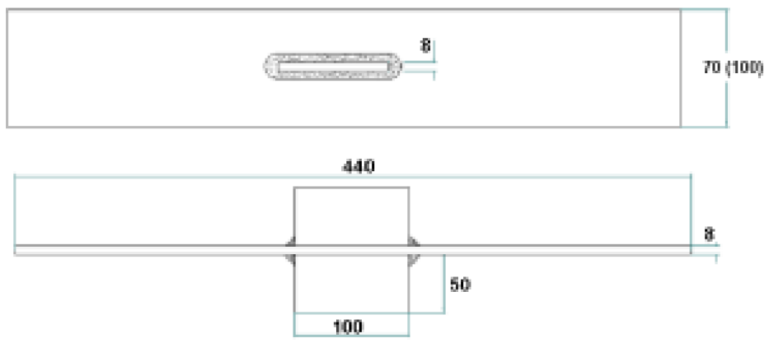

Figure 37: Welded specimens in [36]

For the variable amplitude loading, two types of linear spectrum with an irregularity factor I = 1 were used: the first one with low maximum stress and mean stress equal to half of the maximum stress, the second one with high maximum stress and stress ratio equal to zero. Residual stress measurements were carried out using the X-ray diffraction technique. The objective of the residual stress measurements was to measure the residual stress in the longitudinal direction of the main plate in the as-welded condition, after 50,000 cycles and after 600,000 cycles in order to study the residual stress relaxation due to variable amplitude loading. The measurements were carried out 1-2 mm out from the weld toe at all four weld toe locations on the specimen. Figure 38 shows the results from the measurements of the residual stresses in the vicinity of the weld toe, using the second load spectrum with severe relaxation of residual stress. The results showed that only small residual stress relaxation was observed when the first spectrum was used. This was due to the lower maximum stress levels in the first spectrum.

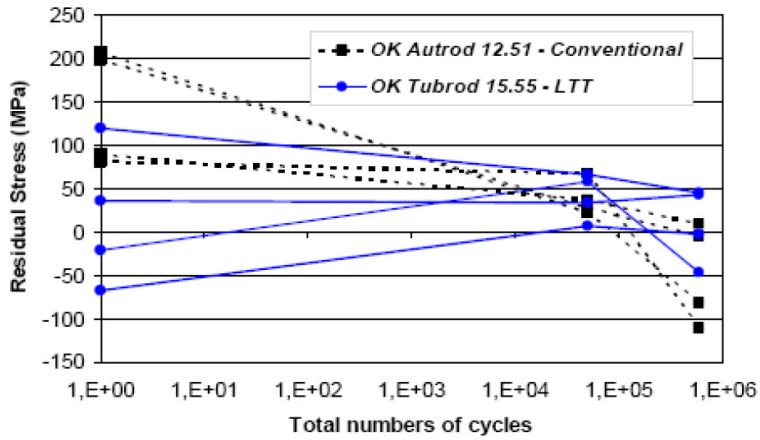

Figure 38: Residual stress relaxation due to variable amplitude fatigue loading using the second load spectrum in [36]

Farajian-Sohi et al (2008) [37] studied the welding residual stress behaviour in welded S235JRG2, S355J2G3 steel butt welded specimens under static and cyclic loading and obtained the correlation between the relaxation and redistribution of the stress field and material mechanical properties. The butt welded specimen is shown in Figure 39. The residual stress measurements were performed using the X-ray diffraction technique.

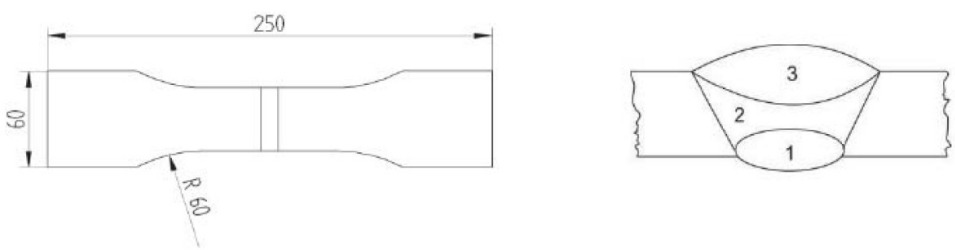

Figure 39: Butt welded specimens in [37]

In cyclic loading the test was stopped after the first half cycle followed by measurement of the residual stress and afterwards the cyclic loading was stopped after 10, 10^2, 10^3, 10^4 cycles and the X-ray measurement was performed. Cyclic loading of the specimens was performed with and without applying mean stresses. It was observed that in the cases where relaxation occurred, the first half cycle played a significant role. After subsequent loading of the specimen until 1000 cycles, the transversal residual stress relaxed only slightly compared with the relaxation in the first half cycle, see Figure 40.

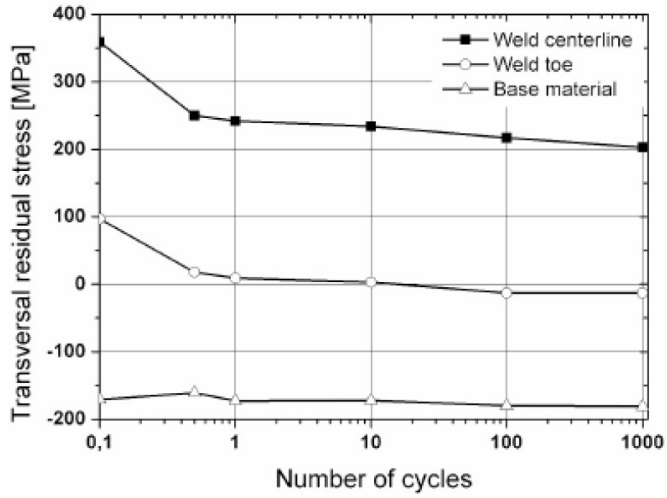

Figure 40: Residual stress relaxation under cyclic loading in [37]

In Figure 41 the von Mises stress at the weld seam centreline is plotted as a function of number of loading cycles for all cyclic loading conditions. The results showed that regardless of what the initial residual stress was, a significant residual stress relaxation with the same relaxation rate was observed in the first cycle for all the loading conditions due to exceeding the monotonic yield strength value of the material. After the first loading cycle it was observed that as long as the calculated von Mises value, which is a function of residual stress, mean stress and loading stress, exceeded the monotonic yield strength, the residual stress relaxation occurred but with a lower rate than that of the first load cycle. When the von Mises stress was between the cyclic and monotonic yield strength, no significant relaxation occurred and the residual stress remained stable.

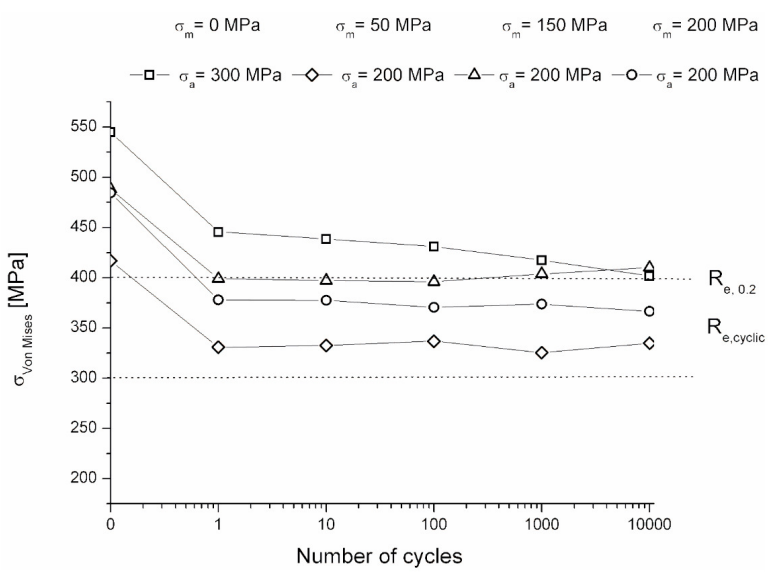

Figure 41: Residual stress relaxation for different cyclic loading conditions in [37]

Farajian et al (2009) [38] studied the relaxation of surface and near surface welding residual stresses in S690QL steel under static and cyclic loading. The butt welded specimens (Figure 39) were loaded using constant amplitude cycles with and without

mean stress. Residual stress was measured using the X-ray diffraction technique. The residual stresses after half a cycle and then in every 10^n cycles were measured. Figure 42 shows the transverse and longitudinal residual stress relaxation under a 400 MPa applied stress amplitude and stress ratio R = -1. The transverse residual stress relaxed significantly at the first half cycle, with the relaxation more pronounced for larger stress amplitudes. After half a cycle of loading the transverse residual stress did not change significantly.

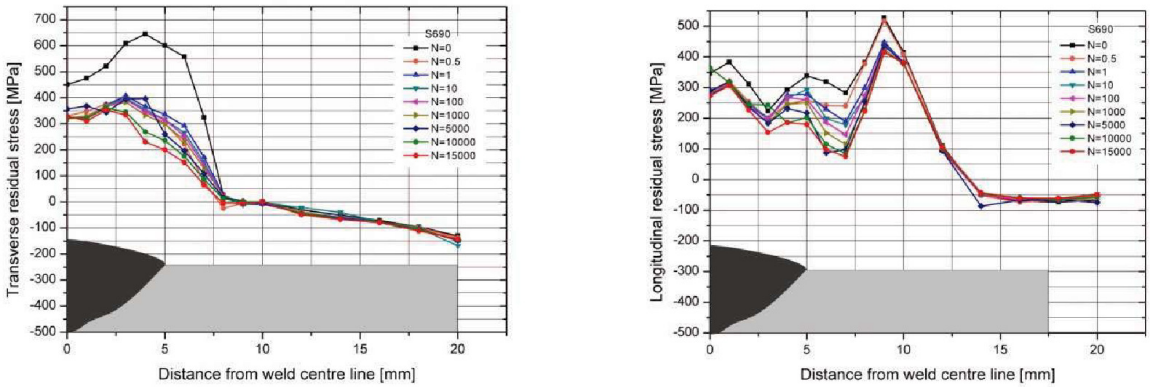

Figure 42: a) Transverse and b) longitudinal cyclic residual stress relaxation, *R* = -1, stress amplitude = 400 MPa in [38]

Polezhayeva (2010) [2] performed fatigue testing on both longitudinal fillet welded plate specimens (Figure 22) and welded panels (Figure 23). The specimens and panels were manufactured from Lloyd's Grade A steel plates with a specified minimum yield strength of 235 MPa. Both constant and variable amplitude loading tests were conducted. Residual stresses introduced by welding were measured. In addition, some measurements were also made after the application of fatigue loading, to determine the extent to which the loading changed the original welding-induced residual stresses. The centre-hole rosette gauge technique was used to measure the residual stresses.

Figure 43 shows the effect of cyclic loading on the residual stresses in the plate and panel specimens. The results showed that the measured residual stress values, in the panels and plate joints in the as-welded condition, were in the range 150 to 400 MPa, close to or above yield. Post weld heat treatment reduced these values to about 20 MPa in the plate specimens. There was strong evidence that the residual stress was partly relaxed (to around 130 MPa) by application of one to ten cycles of fatigue loading. It was also suggested that relaxation of residual stress is more pronounced under tensile loading. Residual stress relaxation due to the applied fatigue loading was beneficial if the subsequent fatigue loading produced stress ranges that were partly compressive.

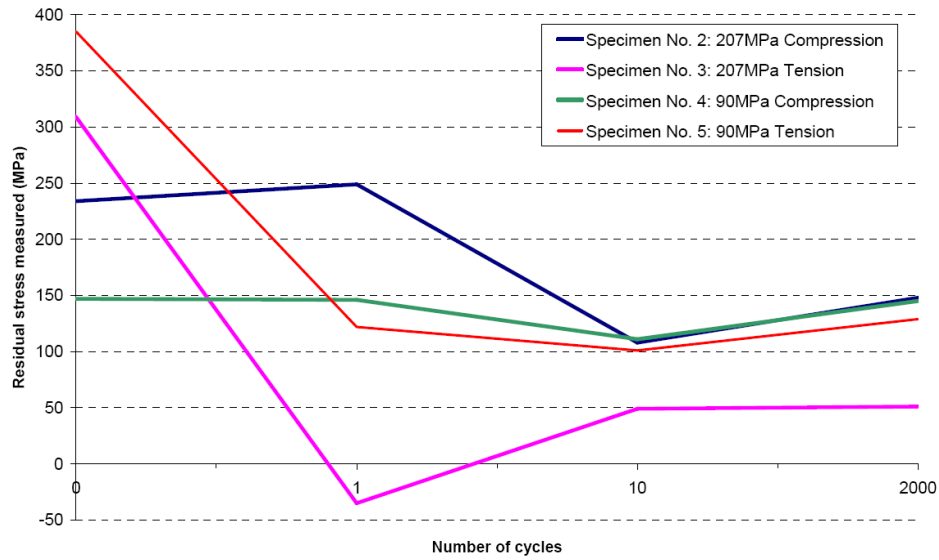

a)

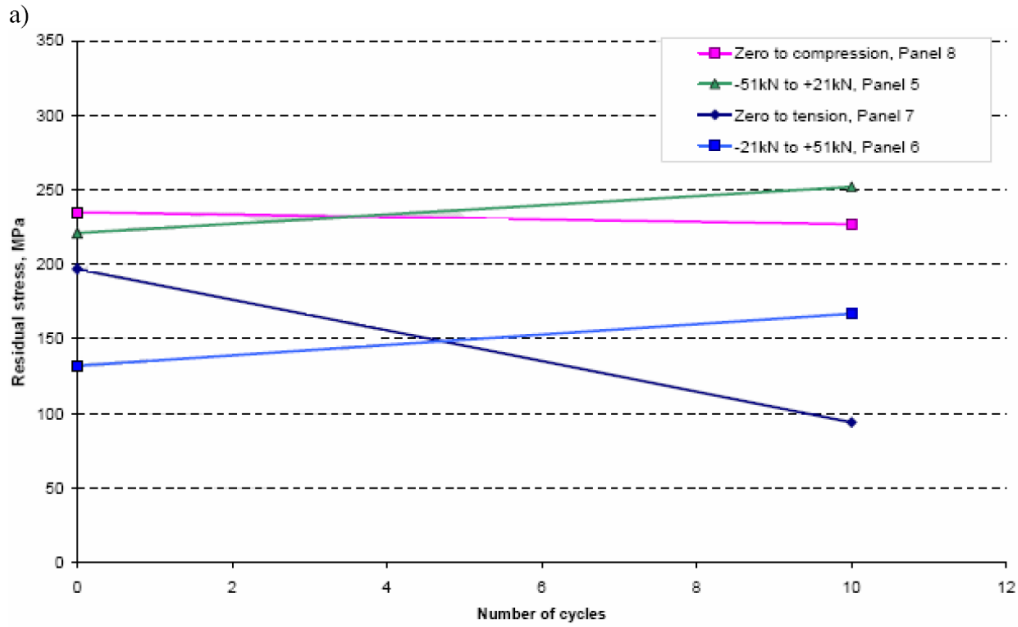

b)

Figure 43: Effect of cyclic loading on the residual stress in the plate and panel specimens in [2]: a) Plate specimens; b) Welded panels

Based on the literature review in this and the previous sections, the following conclusions can be drawn:

Although there is a large scatter for change in residual stress after the application of one or few load cycles, the tendency is that the relaxation increases with the increase of the applied hot spot stress range.

There is an average of 60% reduction in residual stress after the application of a hot spot stress equal to the yield stress of the material, with a lower limit of 20% relaxation. Conservatively, it could be assumed that there is no relaxation in the welding residual

stress if the applied positive hot spot stress is below 0.6 σ_y, and a 20% relaxation if the applied positive hot spot stress is equal to yield.

It is conservative to assume that there is no relaxation occurring under fully compressive stress.

There is not enough data to analyse residual stress relaxation after the application of a partly compressive hot spot stress cycle.

2.5 HOT SPOT STRESSES IN FATIGUE CRITICAL LOCATIONS

Structural members often undergo fairly large static loading before they enter service or variable amplitude cyclic loading when they are in service. The combined effect of both applied stress and high initial residual stress is expected to cause shakedown of the residual stress. In order to identify the level of hot spot stresses at a ship's fatigue critical locations, and therefore have an understanding how residual welding stresses can relax under cargo and ballast static loads, Polezhayeva (2010) [1] carried out the finite element analyses for two tankers and a bulk carrier. A typical fine mesh of a fatigue critical location is shown in Figure 44. The two load cases considered were a static cargo load case and a static ballast load case.

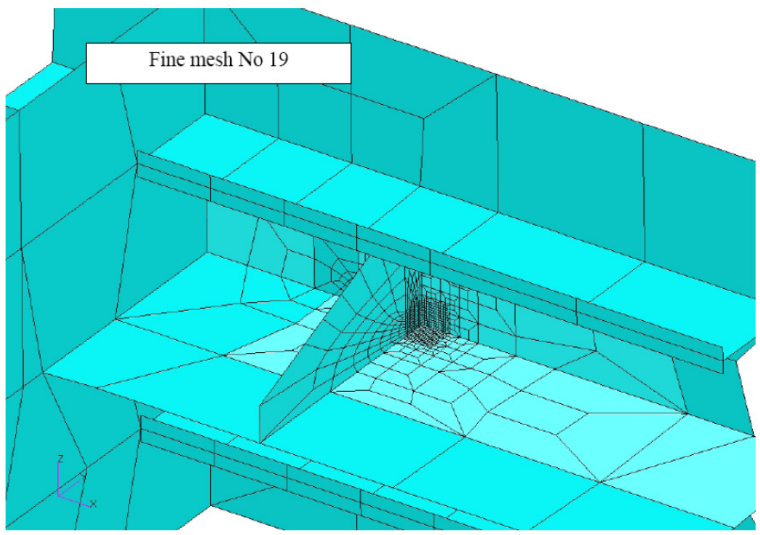

Figure 44: Typical fine mesh of a fatigue critical location [1]

Typical finite element results are shown in Table 3. The results showed that during various ship static load cases, the calculated static or applied mean hot spot stress was equal to or exceeded the magnitude of the yield stress in both tension and compression at various fatigue critical locations. This has to be considered in fatigue assessments. If, for a given loading condition, the static hot spot stress is below negative yield and the residual stress is assumed to be non-relaxed and equal to positive yield, the resulting effective mean hot spot stress will be zero or negative. The fatigue stress range therefore will be 50% or more in compression. Assuming the compressive part of cycle to have a non-damaging effect, the fatigue stress range will be reduced. If, for given loading condition, the static or applied mean hot spot stress is positive and above 0.6 σ_y, then the residual stress should be considered relaxed, according to the previous section, such that for all following load cycles, the mean effective hot spot stress is the sum of the applied hot spot stress and the relaxed residual stress.

Table 3: Finite element results for the bulk carrier in [1]

Loading conditions	Hot spot directional stress , fraction of σ_y					
	Iron Ore (No.4 cargo hold empty)	Coal	Grain	Special Light Ballast	Normal Ballast	Heavy Ballast
Location1 Lower bulkhead stool	1.00	-0.52	-0.45	-3.40	0.79	-3.38
Location1 Lower hopper Knuckle	1.81	0.34	0.32	-2.25	0.25	-2.06
Location 3 Side frame end bracket, weld toe and bracket end	0.74	-0.07	-0.08	-0.99	0.16	-0.96
	1.45	-0.16	-0.17	-2.03	0.29	-1.95
Material Notes Grade A, yield stress 235N/mm						

2.6 FATIGUE TESTS RESULTS DATABASE

Wherever possible, the fatigue tests results from the literature review are summarized in the following tables, according to the major fatigue test parameters, which included the specimen type, weld type, weld direction, heat treatment, material, load history, load direction and stress ratio. In addition, the calculated mean S-N curve parameters, the fatigue enhancement factor calculated with respect to that for R = 0 and the reference of each test are also summarized in the tables wherever possible. The S-N curve parameters summarized in the tables are *C* and *m* in the S-N curve equation:

$$N = C(\Delta\sigma)^m \tag{2}$$

where
N = fatigue life (cycles)
$\Delta\sigma$ = applied stress range (MPa)
C = S-N curve parameter (intercept) (cycles/MPa^m)
m = S-N curve parameter (slope) (dimensionless).

These tables provide a more convenient way to identify where fatigue tests data is lacking and the effects of varying the parameters in the tests.

Table 4: Fatigue tests data for *R* = -infinity

Specimen Type	Heat Treatment	Material	Load History	Loading Mode	Stress Ratio	S-N Curve Slope (*m*)	S-N Curve Intercept (*C*) (cycles/MPa^m)	f(R)	Year	Author
Longitudinal attachment	No Treatment	High Strength Steel	Constant Amplitude	Axial	-infinity	3	1.371E+12	1.25	1982	Maddox
Longitudinal attachment	No Treatment	High Strength Steel	Constant Amplitude	Axial	-infinity	N/A	N/A	N/A	1985	Tilly
Longitudinal attachment	No Treatment	High Strength Steel	Constant Amplitude	Axial	-infinity	N/A	N/A	N/A	2004	Rorup et al
Longitudinal attachment	No Treatment	High Strength Steel	Constant Amplitude	Axial	-infinity	3	3.614E+12	1.46	2000	Rorup et al
Longitudinal attachment	No Treatment	High Strength Steel	Constant Amplitude	Axial	-infinity	3	1.140E+12	1.09	2010	Polezhayeva
Longitudinal attachment	Stress Relieved	High Strength Steel	Constant Amplitude	Axial	-infinity	3	1.860E+13	3.17	2010	Polezhayeva
Longitudinal attachment	No Treatment	High Strength Steel	Variable Amplitude	Axial	-infinity	N/A	N/A	N/A	1985	Tilly
Longitudinal attachment	No Treatment	High Strength Steel	Variable Amplitude	Axial	-infinity	3	2.480E+12	1.27	2010	Polezhayeva

Specimen Type	Heat Treatment	Material	Load History	Loading Mode	Stress Ratio	S-N Curve Slope (*m*)	S-N Curve Intercept (*C*) (cycles/MPa^m)	f(R)	Year	Author
Longitudinal attachment	No Treatment	High Strength Steel	Constant Amplitude	Bending	-infinity	3	1.711E+13	1.28	2010	Polezhayeva
Longitudinal attachment	No Treatment	Aluminium	Constant Amplitude	Axial	-infinity	3	4.120E+11	1.56	N/A	Maddox

Table 5: Fatigue tests data for *R* = -10

Specimen Type	Heat Treatment	Material	Load History	Loading Mode	Stress Ratio	S-N Curve Slope (*m*)	S-N Curve Intercept (*C*) (cycles/MPa^m)	f(R)	Year	Author
Longitudinal attachment	No Treatment	High Strength Steel	Constant Amplitude	Bending	-10	3	1.711E+13	1.28	2010	Polezhayeva

Table 6: Fatigue tests data for *R* = -3

Specimen Type	Heat Treatment	Material	Load History	Loading Mode	Stress Ratio	S-N Curve Slope (*m*)	S-N Curve Intercept (*C*) (cycles/MPa^m)	f(R)	Year	Author
Longitudinal attachment	No Treatment	High Strength Steel	Constant Amplitude	Axial	-3	N/A	N/A	N/A	2004	Rorup et al
Longitudinal attachment	No Treatment	High Strength Steel	Constant Amplitude	Axial	-3	3	1.54E+12	1.10	2000	Rorup et al
Longitudinal attachment	No Treatment	High Strength Steel	Variable Amplitude	Axial	-3	3	3.39E+15	1.88	2000	Rorup et al

Table 7: Fatigue tests data for *R* = -1

Specimen Type	Heat Treatment	Material	Load History	Loading Mode	Stress Ratio	S-N Curve Slope (*m*)	S-N Curve Intercept (*C*) (cycles/MPa^m)	f(R)	Year	Author
Longitudinal attachment	No Treatment	High Strength Steel	Constant Amplitude	Axial	-1	3	8.23E+11	1.06	1982	Maddox
Longitudinal attachment	No Treatment	High Strength Steel	Constant Amplitude	Axial	-1	3	1.34E+12	1.05	2000	Rorup et al
Longitudinal attachment	No Treatment	High Strength Steel	Constant Amplitude	Axial	-1	3	7.70E+11	1.12	1985	Gurney
Longitudinal attachment	No Treatment	High Strength Steel	Constant Amplitude	Axial	-1	3	7.82E+11	1.11	1988	Gurney
Longitudinal attachment	No Treatment	High Strength Steel	Constant Amplitude	Axial	-1	3.00	1.21E+12	1.11	2010	Polezhayeva
Longitudinal attachment	Stress Relieved	High Strength Steel	Constant Amplitude	Axial	-1	3	7.82E+11	1.00	1982	Maddox
Longitudinal attachment	Stress Relieved	High Strength Steel	Constant Amplitude	Axial	-1	3	1.81E+12	1.46	1985	Gurney
Longitudinal attachment	Stress Relieved	High Strength Steel	Constant Amplitude	Axial	-1	3	1.32E+12	N/A	1985	Gurney

Specimen Type	Heat Treatment	Material	Load History	Loading Mode	Stress Ratio	S-N Curve Slope (*m*)	S-N Curve Intercept (*C*) (cycles/MPa^m)	f(R)	Year	Author
Longitudinal attachment	Stress Relieved	High Strength Steel	Constant Amplitude	Axial	-1	2.72	4.33E+11	1.41	1992	Gurney
Longitudinal attachment	Stress Relieved	High Strength Steel	Constant Amplitude	Axial	-1	2.72	4.33E+11	1.41	1992	Gurney
Longitudinal attachment	Stress Relieved	High Strength Steel	Constant Amplitude	Axial	-1	3.00	3.28E+12	1.78	2010	Polezhayeva
Longitudinal attachment	No Treatment	High Strength Steel	Variable Amplitude	Axial	-1	N/A	N/A	N/A	1985	Gurney
Longitudinal attachment	Stress Relieved	High Strength Steel	Variable Amplitude	Axial	-1	N/A	N/A	N/A	1985	Gurney
Longitudinal attachment	Stress Relieved	High Strength Steel	Variable Amplitude	Axial	-1	N/A	N/A	N/A	1985	Gurney
Longitudinal attachment	Stress Relieved	High Strength Steel	Variable Amplitude	Axial	-1	N/A	N/A	N/A	1985	Gurney
Longitudinal attachment	Stress Relieved	High Strength Steel	Variable Amplitude	Axial	-1	N/A	N/A	N/A	1985	Gurney
Longitudinal attachment	Stress Relieved	High Strength Steel	Variable Amplitude	Axial	-1	N/A	N/A	N/A	1985	Gurney

Specimen Type	Heat Treatment	Material	Load History	Loading Mode	Stress Ratio	S-N Curve Slope (*m*)	S-N Curve Intercept (*C*) (cycles/MPa^m)	f(R)	Year	Author
Longitudinal attachment	No Treatment	High Strength Steel	Variable Amplitude	Axial	-1	3	6.46E+14	1.08	2000	Rorup et al
Longitudinal attachment	No Treatment	High Strength Steel	Variable Amplitude	Axial	-1	N/A	N/A	N/A	1988	Gurney
Longitudinal attachment	No Treatment	High Strength Steel	Variable Amplitude	Axial	-1	3.00	1.21E+12	1.00	2010	Polezhayeva
Longitudinal attachment	Stress Relieved	High Strength Steel	Variable Amplitude	Axial	-1	N/A	N/A	N/A	1992	Gurney
Transverse attachment	No Treatment	High Strength Steel	Constant Amplitude	Axial	-1	3.25	6.32E+12	1.04	2003	Sonsino et al
Transverse attachment	Thermo-Mechanically Treated	High Strength Steel	Constant Amplitude	Axial	-1	3.25	5.17E+12	0.76	2003	Sonsino et al
Transverse attachment	Water Quenched	High Strength Steel	Constant Amplitude	Axial	-1	3.25	7.18E+12	0.98	2003	Sonsino et al
Transverse attachment	Water Quenched	High Strength Steel	Constant Amplitude	Axial	-1	3.25	1.89E+13	1.40	2003	Sonsino et al
Transverse attachment	No Treatment	High Strength Steel	Variable Amplitude	Axial	-1	3.25	1.97E+14	N/A	2003	Sonsino et al

Specimen Type	Heat Treatment	Material	Load History	Loading Mode	Stress Ratio	S-N Curve Slope (*m*)	S-N Curve Intercept (*C*) (cycles/MPa^m)	f(R)	Year	Author
Transverse attachment	Thermo-Mechanically Treated	High Strength Steel	Variable Amplitude	Axial	-1	3.25	1.24E+14	N/A	2003	Sonsino et al
Transverse attachment	Thermo-Mechanically Treated	High Strength Steel	Variable Amplitude	Axial	-1	3.25	1.24E+14	N/A	2003	Sonsino et al
Transverse attachment	Water Quenched	High Strength Steel	Variable Amplitude	Axial	-1	3.25	4.21E+14	N/A	2003	Sonsino et al
Transverse attachment	Water Quenched	High Strength Steel	Variable Amplitude	Axial	-1	3.25	4.68E+14	N/A	2003	Sonsino et al
Transverse attachment	Water Quenched	High Strength Steel	Variable Amplitude	Axial	-1	3.25	6.71E+14	N/A	2003	Sonsino et al
Transverse attachment	Water Quenched	High Strength Steel	Variable Amplitude	Axial	-1	3.25	1.04E+15	N/A	2003	Sonsino et al
Butt welded	No Treatment	High Strength Steel	Constant Amplitude	Axial	-1	3.5	1.56E+14	1.34	2003	Sonsino et al
Butt welded	Thermo-Mechanically Treated	High Strength Steel	Constant Amplitude	Axial	-1	3.5	4.28E+14	1.20	2003	Sonsino et al
Butt welded	Water Quenched	High Strength Steel	Constant Amplitude	Axial	-1	3.5	6.49E+13	0.91	2003	Sonsino et al

Specimen Type	Heat Treatment	Material	Load History	Loading Mode	Stress Ratio	S-N Curve Slope (*m*)	S-N Curve Intercept (*C*) (cycles/MPa^m)	f(R)	Year	Author
Butt welded	Water Quenched	High Strength Steel	Constant Amplitude	Axial	-1	3.5	2.26E+14	1.43	2003	Sonsino et al
Butt welded	No Treatment	High Strength Steel	Variable Amplitude	Axial	-1	3.5	1.51E+15	N/A	2003	Sonsino et al
Butt welded	Thermo-Mechanically Treated	High Strength Steel	Variable Amplitude	Axial	-1	3.5	8.31E+15	N/A	2003	Sonsino et al
Butt welded	Thermo-Mechanically Treated	High Strength Steel	Variable Amplitude	Axial	-1	3.5	3.75E+15	N/A	2003	Sonsino et al
Butt welded	Water Quenched	High Strength Steel	Variable Amplitude	Axial	-1	3.5	1.48E+16	N/A	2003	Sonsino et al
Butt welded	Water Quenched	High Strength Steel	Variable Amplitude	Axial	-1	3.5	2.14E+15	N/A	2003	Sonsino et al
Butt welded	Water Quenched	High Strength Steel	Variable Amplitude	Axial	-1	3.5	6.76E+15	N/A	2003	Sonsino et al
Butt welded	Water Quenched	High Strength Steel	Variable Amplitude	Axial	-1	3.5	1.67E+15	N/A	2003	Sonsino et al
Transverse attachment	Thermo-Mechanically Treated	High Strength Steel	Constant Amplitude	Bending	-1	3.25	1.48E+13	1.05	2003	Sonsino et al

Specimen Type	Heat Treatment	Material	Load History	Loading Mode	Stress Ratio	S-N Curve Slope (*m*)	S-N Curve Intercept (*C*) (cycles/MPa^m)	f(R)	Year	Author
Transverse attachment	Water Quenched	High Strength Steel	Constant Amplitude	Bending	-1	3.25	4.27E+13	1.00	2003	Sonsino et al
Transverse attachment	No Treatment	High Strength Steel	Variable Amplitude	Bending	-1	3.25	4.60E+14	N/A	2003	Sonsino et al
Transverse attachment	Thermo-Mechanically Treated	High Strength Steel	Variable Amplitude	Bending	-1	3.25	3.71E+14	0.93	2003	Sonsino et al
Transverse attachment	Thermo-Mechanically Treated	High Strength Steel	Variable Amplitude	Bending	-1	3.25	3.44E+14	N/A	2003	Sonsino et al
Transverse attachment	Water Quenched	High Strength Steel	Variable Amplitude	Bending	-1	3.25	9.80E+14	0.88	2003	Sonsino et al
Transverse attachment	Water Quenched	High Strength Steel	Variable Amplitude	Bending	-1	3.25	1.48E+15	0.98	2003	Sonsino et al
Butt welded	No Treatment	High Strength Steel	Constant Amplitude	Bending	-1	3.5	2.18E+14	N/A	2003	Sonsino et al
Butt welded	Thermo-Mechanically Treated	High Strength Steel	Constant Amplitude	Bending	-1	3.5	9.06E+13	1.03	2003	Sonsino et al
Butt welded	Water Quenched	High Strength Steel	Constant Amplitude	Bending	-1	3.5	2.43E+14	1.03	2003	Sonsino et al

Specimen Type	Heat Treatment	Material	Load History	Loading Mode	Stress Ratio	S-N Curve Slope (*m*)	S-N Curve Intercept (*C*) (cycles/MPa^m)	f(R)	Year	Author
Butt welded	No Treatment	High Strength Steel	Variable Amplitude	Bending	-1	3.5	3.19E+15	N/A	2003	Sonsino et al
Butt welded	Thermo-Mechanically Treated	High Strength Steel	Variable Amplitude	Bending	-1	3.5	3.14E+15	0.94	2003	Sonsino et al
Butt welded	Thermo-Mechanically Treated	High Strength Steel	Variable Amplitude	Bending	-1	3.5	2.22E+15	N/A	2003	Sonsino et al
Butt welded	Water Quenched	High Strength Steel	Variable Amplitude	Bending	-1	3.5	3.57E+15	0.94	2003	Sonsino et al
Butt welded	Water Quenched	High Strength Steel	Variable Amplitude	Bending	-1	3.5	3.63E+15	0.67	2003	Sonsino et al
Longitudinal attachment	No Treatment	High Strength Steel	Constant Amplitude	Bending	-1	3.00	8.076E+12	1.00	2010	Polezhayeva
Longitudinal attachment	No Treatment	Aluminium	Constant Amplitude	Axial	-1	3	1.08E+11	1.00	N/A	Maddox
Longitudinal attachment	No Treatment	Aluminium	Constant Amplitude	Axial	-1	N/A	N/A	N/A	N/A	Maddox

Table 8: Fatigue tests data for R = -0.33

Specimen Type	Heat Treatment	Material	Load History	Loading Mode	Stress Ratio	S-N Curve Slope (m)	S-N Curve Intercept (C) (cycles/MPa^m)	f(R)	Year	Author
Longitudinal attachment	No Treatment	High Strength Steel	Constant Amplitude	Axial	-0.33	N/A	N/A	N/A	2004	Rorup et al

Table 9: Fatigue tests data for $R = 0$

Specimen Type	Heat Treatment	Material	Load History	Loading Mode	Stress Ratio	S-N Curve Slope (m)	S-N Curve Intercept (C) (cycles/MPa^m)	f(R)	Year	Author
Longitudinal attachment	No Treatment	High Strength Steel	Constant Amplitude	Axial	0	3	6.94E+11	1.00	1982	Maddox
Longitudinal attachment	No Treatment	High Strength Steel	Constant Amplitude	Axial	0	N/A	N/A	N/A	2004	Rorup et al
Longitudinal attachment	No Treatment	High Strength Steel	Constant Amplitude	Axial	0	3	1.16E+12	1.00	2000	Rorup et al
Longitudinal attachment	No Treatment	High Strength Steel	Constant Amplitude	Axial	0	3	5.48E+11	1.00	1985	Gurney
Longitudinal attachment	No Treatment	High Strength Steel	Constant Amplitude	Axial	0	3	5.68E+11	1.00	1985	Gurney
Longitudinal attachment	No Treatment	High Strength Steel	Constant Amplitude	Axial	0	3	5.68E+11	1.00	1988	Gurney
Longitudinal attachment	No Treatment	High Strength Steel	Constant Amplitude	Axial	0	2.62	1.01E+11	1.00	1992	Gurney
Longitudinal attachment	Stress Relieved	High Strength Steel	Constant Amplitude	Axial	0	3	5.86E+11	1.00	1985	Gurney

Specimen Type	Heat Treatment	Material	Load History	Loading Mode	Stress Ratio	S-N Curve Slope (*m*)	S-N Curve Intercept (*C*) (cycles/MPa^m)	f(R)	Year	Author
Longitudinal attachment	Stress Relieved	High Strength Steel	Constant Amplitude	Axial	0	3.00	5.68E+11	1.00	1992	Gurney
Longitudinal attachment	No Treatment	High Strength Steel	Variable Amplitude	Axial	0	N/A	N/A	N/A	1985	Gurney
Longitudinal attachment	No Treatment	High Strength Steel	Variable Amplitude	Axial	0	N/A	N/A	N/A	1985	Gurney
Longitudinal attachment	No Treatment	High Strength Steel	Variable Amplitude	Axial	0	3.65	N/A	N/A	1985	Gurney
Longitudinal attachment	No Treatment	High Strength Steel	Variable Amplitude	Axial	0	3	5.12E+14	1.00	2000	Rorup et al
Longitudinal attachment	No Treatment	High Strength Steel	Variable Amplitude	Axial	0	N/A	N/A	N/A	1985	Gurney
Longitudinal attachment	No Treatment	High Strength Steel	Variable Amplitude	Axial	0	N/A	N/A	N/A	1988	Gurney
Longitudinal attachment	No Treatment	High Strength Steel	Variable Amplitude	Axial	0	N/A	N/A	N/A	1992	Gurney
Longitudinal attachment	No Treatment	High Strength Steel	Variable Amplitude	Axial	0	3.00	1.21E+12	1.00	2010	Polezhayeva

Specimen Type	Heat Treatment	Material	Load History	Loading Mode	Stress Ratio	S-N Curve Slope (*m*)	S-N Curve Intercept (*C*) (cycles/MPa^m)	f(R)	Year	Author
Longitudinal attachment	Stress Relieved	High Strength Steel	Variable Amplitude	Axial	0	N/A	N/A	N/A	1992	Gurney
Transverse attachment	No Treatment	High Strength Steel	Constant Amplitude	Axial	0	3.25	5.54E+12	1.00	2003	Sonsino et al
Transverse attachment	Thermo-Mechanically Treated	High Strength Steel	Constant Amplitude	Axial	0	3.25	1.27E+13	1.00	2003	Sonsino et al
Transverse attachment	Water Quenched	High Strength Steel	Constant Amplitude	Axial	0	3.25	7.64E+12	1.00	2003	Sonsino et al
Transverse attachment	Water Quenched	High Strength Steel	Constant Amplitude	Axial	0	3.25	6.32E+12	1.00	2003	Sonsino et al
Butt welded	No Treatment	High Strength Steel	Constant Amplitude	Axial	0	3.5	5.57E+13	1.00	2003	Sonsino et al
Butt welded	Thermo-Mechanically Treated	High Strength Steel	Constant Amplitude	Axial	0	3.5	2.26E+14	1.00	2003	Sonsino et al
Butt welded	Water Quenched	High Strength Steel	Constant Amplitude	Axial	0	3.5	9.06E+13	1.00	2003	Sonsino et al
Butt welded	Water Quenched	High Strength Steel	Constant Amplitude	Axial	0	3.5	6.49E+13	1.00	2003	Sonsino et al

Specimen Type	Heat Treatment	Material	Load History	Loading Mode	Stress Ratio	S-N Curve Slope (*m*)	S-N Curve Intercept (*C*) (cycles/MPa^m)	f(R)	Year	Author
Transverse attachment	No Treatment	High Strength Steel	Constant Amplitude	Bending	0	3.25	2.07E+13	1.00	2003	Sonsino et al
Transverse attachment	Thermo-Mechanically Treated	High Strength Steel	Constant Amplitude	Bending	0	3.25	1.27E+13	1.00	2003	Sonsino et al
Transverse attachment	Water Quenched	High Strength Steel	Constant Amplitude	Bending	0	3.25	4.27E+13	1.00	2003	Sonsino et al
Transverse attachment	Thermo-Mechanically Treated	High Strength Steel	Variable Amplitude	Bending	0	3.25	4.76E+14	1.00	2003	Sonsino et al
Transverse attachment	Water Quenched	High Strength Steel	Variable Amplitude	Bending	0	3.25	1.46E+15	1.00	2003	Sonsino et al
Transverse attachment	Water Quenched	High Strength Steel	Variable Amplitude	Bending	0	3.25	1.59E+15	1.00	2003	Sonsino et al
Butt welded	Thermo-Mechanically Treated	High Strength Steel	Constant Amplitude	Bending	0	3.5	8.27E+13	1.00	2003	Sonsino et al
Butt welded	Water Quenched	High Strength Steel	Constant Amplitude	Bending	0	3.5	2.18E+14	1.00	2003	Sonsino et al
Butt welded	Thermo-Mechanically Treated	High Strength Steel	Variable Amplitude	Bending	0	3.5	3.93E+15	1.00	2003	Sonsino et al

Specimen Type	Heat Treatment	Material	Load History	Loading Mode	Stress Ratio	S-N Curve Slope (*m*)	S-N Curve Intercept (*C*) (cycles/MPa^m)	f(R)	Year	Author
Butt welded	Water Quenched	High Strength Steel	Variable Amplitude	Bending	0	3.5	4.37E+15	1.00	2003	Sonsino et al
Butt welded	Water Quenched	High Strength Steel	Variable Amplitude	Bending	0	3.5	1.45E+16	1.00	2003	Sonsino et al
Longitudinal attachment	No Treatment	Aluminium	Constant Amplitude	Axial	0	3	1.08E+11	1.00	N/A	Maddox

Table 10: Fatigue tests data for R = 0.1

Specimen Type	Heat Treatment	Material	Load History	Loading Mode	Stress Ratio	S-N Curve Slope (m)	S-N Curve Intercept (C) (cycles/MPa^m)	f(R)	Year	Author
Longitudinal attachment	No Treatment	High Strength Steel	Constant Amplitude	Axial	0.1	3.00	8.77E+11	1.00	2010	Polezhayeva
Longitudinal attachment	Stress Relieved	High Strength Steel	Constant Amplitude	Axial	0.1	3.00	5.84E+11	1.00	2010	Polezhayeva
Longitudinal attachment	No Treatment	High Strength Steel	Constant Amplitude	Bending	0.1	3.00	8.076E+12	1.00	2010	Polezhayeva
Longitudinal attachment	No Treatment	High Strength Steel	Constant Amplitude	Bending	0.1	3.00	8.076E+12	1.00	2010	Polezhayeva

Table 11: Fatigue tests data for R = 0.25

Specimen Type	Heat Treatment	Material	Load History	Loading Mode	Stress Ratio	S-N Curve Slope (m)	S-N Curve Intercept (C) (cycles/MPa^m)	f(R)	Year	Author
Longitudinal attachment	No Treatment	Aluminium	Constant Amplitude	Axial	0.25	N/A	N/A	N/A	N/A	Maddox

Table 12: Fatigue tests data for R = 0.5

Specimen Type	Heat Treatment	Material	Load History	Loading Mode	Stress Ratio	S-N Curve Slope (m)	S-N Curve Intercept (C) (cycles/MPa^m)	f(R)	Year	Author
Longitudinal attachment	No Treatment	High Strength Steel	Constant Amplitude	Axial	0.5	3	6.94E+11	1.00	1982	Maddox
Longitudinal attachment	No Treatment	High Strength Steel	Constant Amplitude	Axial	0.5	2.82	2.23E+11	0.99	1992	Gurney
Longitudinal attachment	Stress Relieved	High Strength Steel	Constant Amplitude	Axial	0.5	3	7.82E+11	1.00	1982	Maddox

Table 13: Fatigue tests data for R = 0.67

Specimen Type	Heat Treatment	Material	Load History	Loading Mode	Stress Ratio	S-N Curve Slope (m)	S-N Curve Intercept (C) (cycles/MPa^m)	f(R)	Year	Author
Longitudinal attachment	No Treatment	High Strength Steel	Constant Amplitude	Axial	0.67	3	6.94E+11	1.00	1982	Maddox
Longitudinal attachment	Stress Relieved	High Strength Steel	Constant Amplitude	Axial	0.67	3	7.82E+11	1.00	1982	Maddox

Table 14: Fatigue tests data for R = 0.75

Specimen Type	Heat Treatment	Material	Load History	Loading Mode	Stress Ratio	S-N Curve Slope (m)	S-N Curve Intercept (C) (cycles/MPa^m)	f(R)	Year	Author
Longitudinal attachment	No Treatment	High Strength Steel	Constant Amplitude	Axial	0.75	N/A	N/A	N/A	1992	Gurney

Table 15: Fatigue tests data for *R* = Other

Specimen Type	Heat Treatment	Material	Load History	Loading Mode	Stress Ratio	S-N Curve Slope (*m*)	S-N Curve Intercept (*C*) (cycles/MPa^m)	f(R)	Year	Author
Longitudinal attachment	No Treatment	High Strength Steel	Constant Amplitude	Axial	Variable	2.22	8.36E+09	N/A	1992	Gurney
Longitudinal attachment	No Treatment	High Strength Steel	Variable Amplitude	Axial	Stalactitic	N/A	N/A	N/A	1992	Gurney
Longitudinal attachment	No Treatment	High Strength Steel	Variable Amplitude	Axial	Constant tensile mean stress +20 MPa	3.00	1.21E+12	1.00	2010	Polezhayeva
Longitudinal attachment	No Treatment	High Strength Steel	Variable Amplitude	Axial	Constant compressive mean stress -20 MPa	3.00	1.21E+12	1.00	2010	Polezhayeva
Longitudinal attachment	No Treatment	High Strength Steel	Variable Amplitude	Axial	Constant tensile max stress +40 MPa	3.00	1.21E+12	1.00	2010	Polezhayeva
Longitudinal attachment	No Treatment	High Strength Steel	Variable Amplitude	Axial	Constant tensile max stress +20 MPa	3.00	1.21E+12	1.00	2010	Polezhayeva
Longitudinal attachment	No Treatment	High Strength Steel	Variable Amplitude	Bending	Predominantly tensile stress	3.00	8.076E+12	1.00	2010	Polezhayeva
Longitudinal attachment	No Treatment	High Strength Steel	Variable Amplitude	Bending	Predominantly compressive stress	3.00	8.076E+12	1.00	2010	Polezhayeva

2.7 MEAN STRESS MODELS

Fatigue life is dependent on the ratio of the mean stress to alternating stress in the fatigue cycles. Three of the earliest simple mean stress models for assessing the mean stress effect [45] are summarized in Table 16. These models calculate an equivalent stress in terms of the applied alternating stress, the applied mean stress and the yield strength or the ultimate strength of the material. The earliest model, the Gerber model, does not distinguish between compressive and tensile mean stress. The Goodman model is the most commonly used, which typically results in conservative estimates and provides a good fit of the fatigue tests on metals with low-ductility. The Soderberg model is the most conservative and often gives results similar to the Goodman model.

Table 16: Three of the earliest simple mean stress models

Model	Equivalent Stress Formula	Remarks
Gerber (1874)	$\sigma_{eq} = \dfrac{\sigma_a}{1-\left(\dfrac{\sigma_m}{\sigma_u}\right)^2}$	Does not distinguish between compressive and tensile mean stress
Goodman (1899)	$\sigma_{eq} = \dfrac{\sigma_a}{1-\dfrac{\sigma_m}{\sigma_u}}$	Most commonly used, typically results in conservative estimates, and provides good fit of fatigue tests on metals with low-ductility
Soderberg (1930)	$\sigma_{eq} = \dfrac{\sigma_a}{1-\dfrac{\sigma_m}{\sigma_y}}$	Most conservative model, often similar to Goodman

$\sigma_{eq} = equivalent\ stress$ $\quad$ $\sigma_a = applied\ alternating\ stress$

$\sigma_m = mean\ stress$ $\quad$ $\sigma_y = yield\ strength$ $\quad$ $\sigma_u = ultimate\ strength$

Figure 45 and Figure 46 compare the models using HY 80 steel and WT 300 steel, respectively. It can be seen that the differences between the Goodman and the Soderberg models are insignificant for high-strength steel, or when $\sigma_y \approx \sigma_u$.

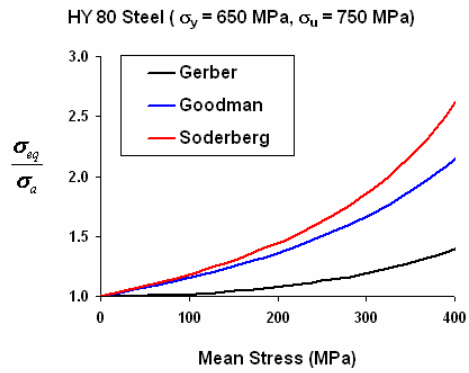

Figure 45: Comparison of three simple mean stress models using HY 80 steel

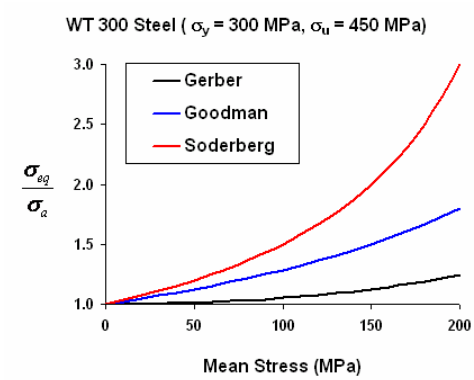

Figure 46: Comparison of three simple mean stress models using WT 300 steel

Further experimental data for structural materials given by Heywood, 1962; Frost et al, 1974; Serensen et al.,1975; Reemsnyder,1995, etc. [46] demonstrated the diversity of fatigue behavior of materials which Goodman's formula was not capable of predicting. A series of proposals were developed that were applicable to particular materials. Heywood suggested a correction to the Goodman's equation:

$$\sigma_a = \left[1 - \left(\frac{\sigma_m}{\sigma_u}\right)\right]\left[\sigma_{eq} + \gamma(\sigma_u - \sigma_{eq})\right] \tag{3}$$

where $\gamma = (\sigma_m / 3\sigma_u)(2 + \sigma_m / 3\sigma_u)$ for steel

$\gamma = (\sigma_m / \sigma_u)/\left(1 + (\log N_o \sigma_u / 2200)^4\right)$ for aluminum

N_o = Number of cycles corresponding to fatigue limit

Other simple mean stress models include the Morrow and SWT (Smith, Watson, Tupper) models based on strain-life approach to fatigue design:

$$\sigma_{\max}\varepsilon_a = \text{constant} = (\sigma_a \varepsilon_a)_{R=-1} \tag{4}$$

and the Walker model:

$$\sigma_{eq} = \sigma_a \left(\frac{2}{1-R}\right)^{1-w} \tag{5}$$

The simple mean stress models presented above apply to non-welded structures only. In welded structures, it is generally accepted that the tensile residual stresses along weld toes reach the yield level and hence, fatigue stresses cycle downward from yield. In addition, compressive applied stress cycles are considered to be partly damaging, with design codes allowing for the reduction in the compressive portion of the applied stress range. Furthermore, S-N design curves are independent of the mean stress.

Due to high residual stresses at welds (in the order of σ_y), fatigue stresses cycle downward from σ_y, regardless of the mean stress value, as shown in Figure 47. Recall the SWT model states that:

$$\sigma_{eq} = f\,(\text{stress range, maximum stress}) \tag{6}$$

In welded structures, $\sigma_{\max} = \sigma_y$, regardless of mean stress. Therefore, fatigue in welded structures with high residual stresses is dependent only on the stress range.

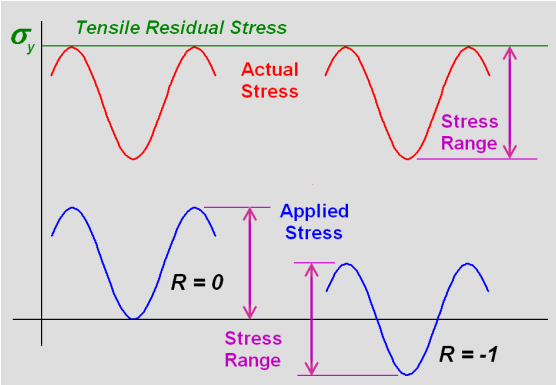

Figure 47: Effect of tensile residual stress on applied stress range

Various design codes consider the mean stress effects in welded structures. The Health and Safety Executive Guidance states that the Effective stress range = Tensile range + 0.6 Compressive range, where the tensile range is equal to the yield stress, as shown in Figure 48.

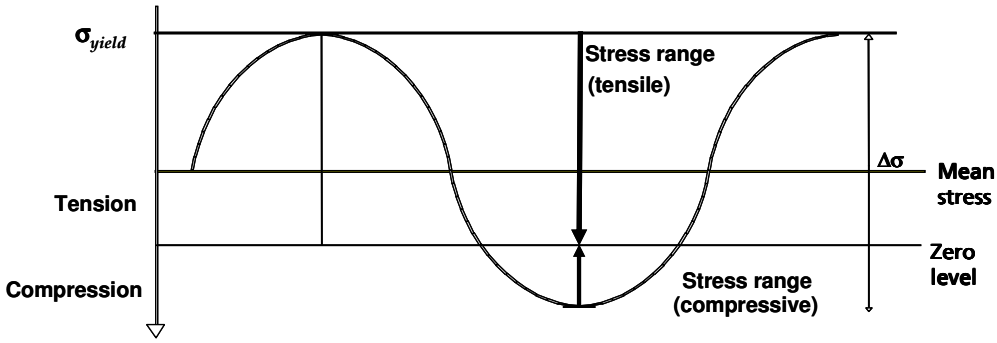

Figure 48: Components of a fatigue stress cycle

DNV's RP C203 & CN 30.7 [47] allow for reductions in stress range similar to the HSE approach. However, the level of reduction depends on the magnitude of residual stresses, as shown in Figure 49. For base material, not significantly affected by residual stresses, the reduction factor in stress range, f_m, is given by:

$$f_m = \frac{\sigma_t + 0.6|\sigma_c|}{\sigma_t + |\sigma_c|} \tag{7}$$

For welded material with residual stresses relieved by high tensile stresses due to external loading:

$$f_m = \frac{\sigma_t + 0.7|\sigma_c|}{\sigma_t + |\sigma_c|} \tag{8}$$

where $\sigma_t = \sigma_{mean} + \frac{\Delta\sigma}{2}$ and $\sigma_c = \sigma_{mean} - \frac{\Delta\sigma}{2}$.

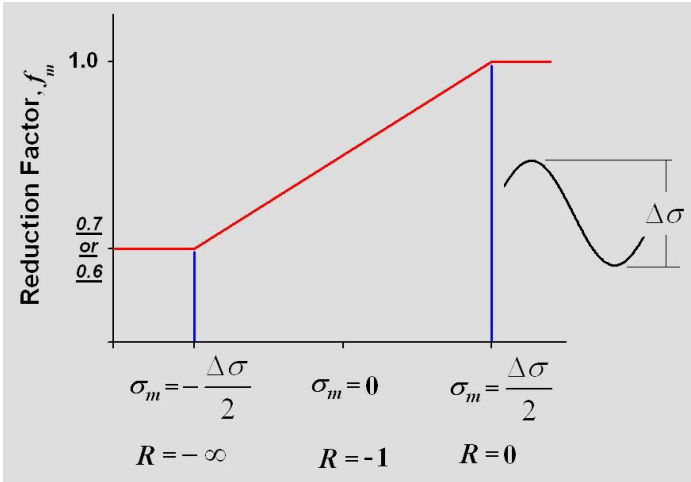

Figure 49: Reduction in stress range according to DNV's RP C203 & CN 30.7

However, Lotsberg [48] found the above reduction factor to be non-conservative and suggested the reduction in the compressive range to be increased to 0.8, such that:

$$f_m = \frac{\sigma_t + 0.8|\sigma_c|}{\sigma_t + |\sigma_c|} \tag{9}$$

It is stated in the ABS guidance notes [49] that if it can be conclusively established that the detail under consideration is always subject to a mean stress of σ_m, the total cumulative damage D is to be adjusted by a factor k_{ms}.

k_{ms}	=	a factor for mean stress effect, which is		(10)
	=	1.0	for $\sigma_m > s_4/2$	
	=	$0.85 + 0.3\sigma_m / s_4$	for $-s_4/2 \le \sigma_m \le s_4/2$	
	=	0.7	for $\sigma_m < -s_4/2$	
s_4	=	long-term stress range corresponding to the representative probability level of 10^{-4}.		

3.0 DEVELOPMENT OF AN APPROPRIATE FATIGUE MODEL

3.1 DESCRIPTION OF THE PROPOSED FATIGUE MODEL

The effect of mean stress on fatigue strength of welded small specimens and structural components under constant and variable amplitude fatigue loading has been reviewed in this work. Based on the literature review the following conclusions can be drawn:

The compressive part of a fatigue cycle is only partly damaging, but down to a stress ratio of $R = -1$, the compressive part has no significant benefit on the fatigue strength. This conclusion applies to the welded joints with severe stress concentrations typical of ship details under constant and variable amplitude fatigue loading.

Under fully compressive applied stress range, the enhancement factor on fatigue strength (f(R)) varied widely from 1.17 to 1.48. Based on the current investigation and literature search, the enhancement factor on fatigue can be conservatively assumed to be 1.2 for fully compressive cycles.

There is not much data on the benefit of partly compressive cycles where the compressive part of the cycle is larger than the tensile part (i.e. stress ratios between $R = -1$ and $R = -\infty$). However, there is an indication that the mean stress influences the fatigue strength of welded joints under variable amplitude loading typical for ships. Therefore, it is proposed to use linear interpolation for partly compressive cycles: The fatigue enhancement factor increases from 1.0 for $R = -1$ (50% compression) to 1.2 for $R = -\infty$ (100% compression) in the loading history. The proposed enhancement factor on fatigue strength, to be used for simplified fatigue assessments, is given by:

$$
\begin{aligned}
f(R_c) &= 1.0 && \text{for } R_c < 0.5 \qquad (11)\\
&= 1.0 + 0.2\left(\frac{R_c - 0.5}{0.5}\right) && \text{for } 0.5 \le R_c < 1\\
&= 1.2 && \text{for } 1 \le R_c\\
R_c &= \text{the fraction of the stress range that is compressive}\\
&= \frac{0 - \sigma_{\min}}{\Delta\sigma}
\end{aligned}
$$

3.2 ANALYSES OF FATIGUE TEST DATA

In welded details, the tensile residual stress at a hot spot is very large and close to the yield stress. Therefore, the actual stresses acting in the vicinity of hot spot are considered to be fluctuating downward from the yield stress irrespective of the mean stress. If a hot spot region is subjected to a tensile stress, which causes local yielding at the hot spot region, the residual stress would be reduced. On the other hand, the compressive part of a fatigue cycle is assumed to be partly damaging, which means a fatigue cycle that is partly compressive is less damaging than one that is entirely tensile. This so-called mean stress effect on the compressive part of the fatigue cycle can be modelled using a mean stress correction factor (g_m) to modify the nominal applied stress range used in the SN curve:

$$N_m = C(g_m \Delta\sigma)^m \tag{12}$$

where g_m is the mean stress correction factor, N_m is the fatigue life with the mean stress effect taken into account, $\Delta\sigma$ is the applied stress range and C and m are the SN curve constants. In other words, the fatigue life with the mean stress effect taken into account is determined from the SN curve using the mean stress corrected applied stress range. The modelling of the mean stress effect using the mean stress correction factor is illustrated in Figure 50.

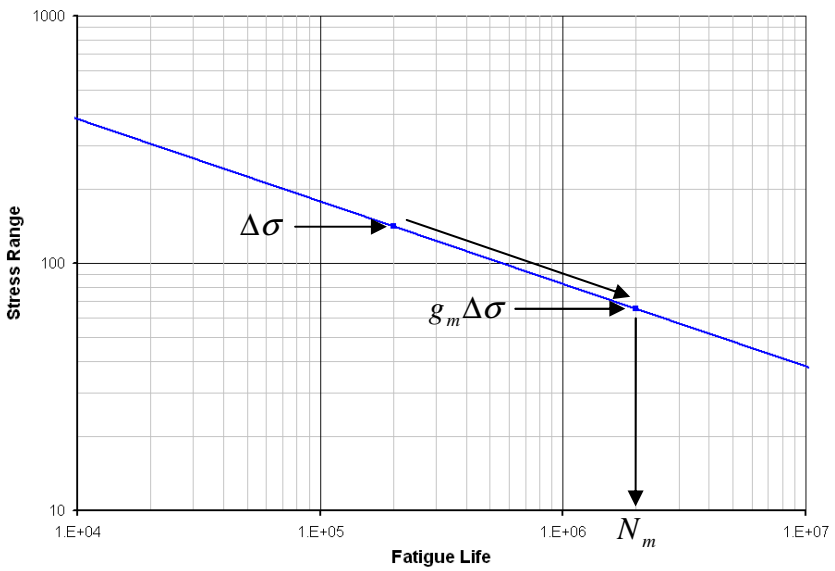

Figure 50: Illustration of the Modelling of the Mean Stress Effect using the Mean Stress Correction Factor

The fatigue test results from various sources [2, 3, 6, 8, 10] were analyzed to compare the effectiveness of the DNV [47], Lotsberg [48], ABS [49] and the proposed [1] models in predicting the mean stress correction factor under both constant amplitude and variable amplitude loading. The mean stress correction factor can be calculated from the above models as follows:

$g_m = f_m$ for the DNV and Lotsberg models,

$g_m = (k_{ms})^{-1/m}$ for the ABS model,

$g_m = 1/\mathrm{f}(R)$ for the proposed model.

Figure 51 and Figure 52 plot the predicted mean stress correction factors against the experimental mean stress correction factors. The solid line indicates where the predicted factor is equal to the experimental factor, such that predictions that are above the line are conservative. The dashed lines indicate the scatter band for the prediction within which the predicted fatigue life is within a factor of two of the experimental fatigue life.

Figure 51 plots the results for constant amplitude loading. It can be seen that the DNV predictions were unconservative in most of the tests. Still, most of the predictions stayed within the scatter band. Meanwhile, the Lotsberg's modification to the DNV model resulted in more conservative predictions and brought all the predictions inside the scatter band. The ABS predictions were even more conservative than the Lotsberg predictions. The ABS predictions were mostly conservative, especially for the fully compressive fatigue cycles. Lastly, the proposed model predictions were the most conservative, especially for the alternating stress cycles ($R = -1$), while having all the predictions inside the scatter band.

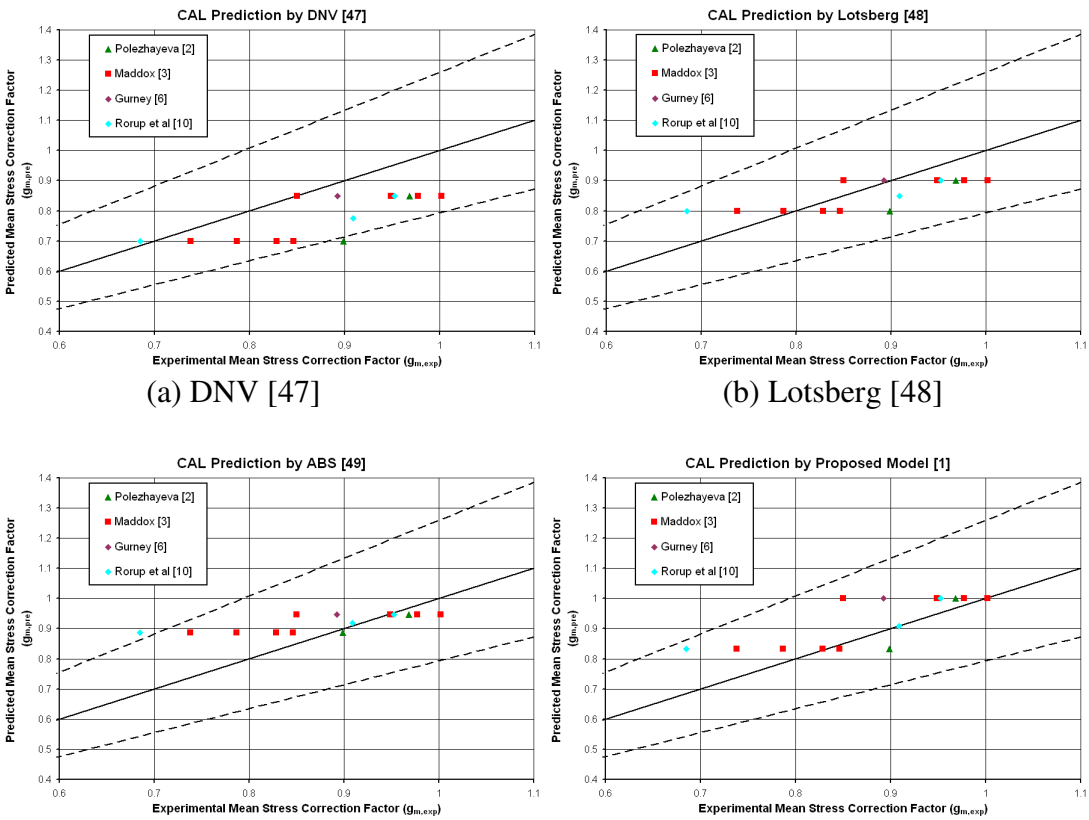

(a) DNV [47] (b) Lotsberg [48]

(c) ABS [49] (d) Proposed [1]

Figure 51: Comparison of the Predicted to the Experimental Mean Stress Correction Factors under Constant Amplitude Loading

Figure 52 plots the results for variable amplitude loading. Equivalent stresses were calculated in order to be used in the models. The equivalent stresses (σ_{eq}) were based on the Miner linear damage rule and given by:

$$\sigma_{eq} = \left(\frac{\Sigma \sigma_i^{-m} \cdot n_i}{\Sigma n_i} \right)^{-1/m} \tag{13}$$

where n_i is the number of cycles at stress range σ_i in the applied variable amplitude loading.

It can be seen that both the DNV and Lotsberg predictions were mostly unconservative but stayed inside the scatter band. The Lotsberg predictions were again more conservative than the DNV predictions. Thus, these test data further validate the Lotsberg's modification to the DNV model. The ABS predictions were again more conservative than the Lotsberg predictions. Lastly, the proposed predictions were again the most conservative and had all the predictions inside the scatter band.

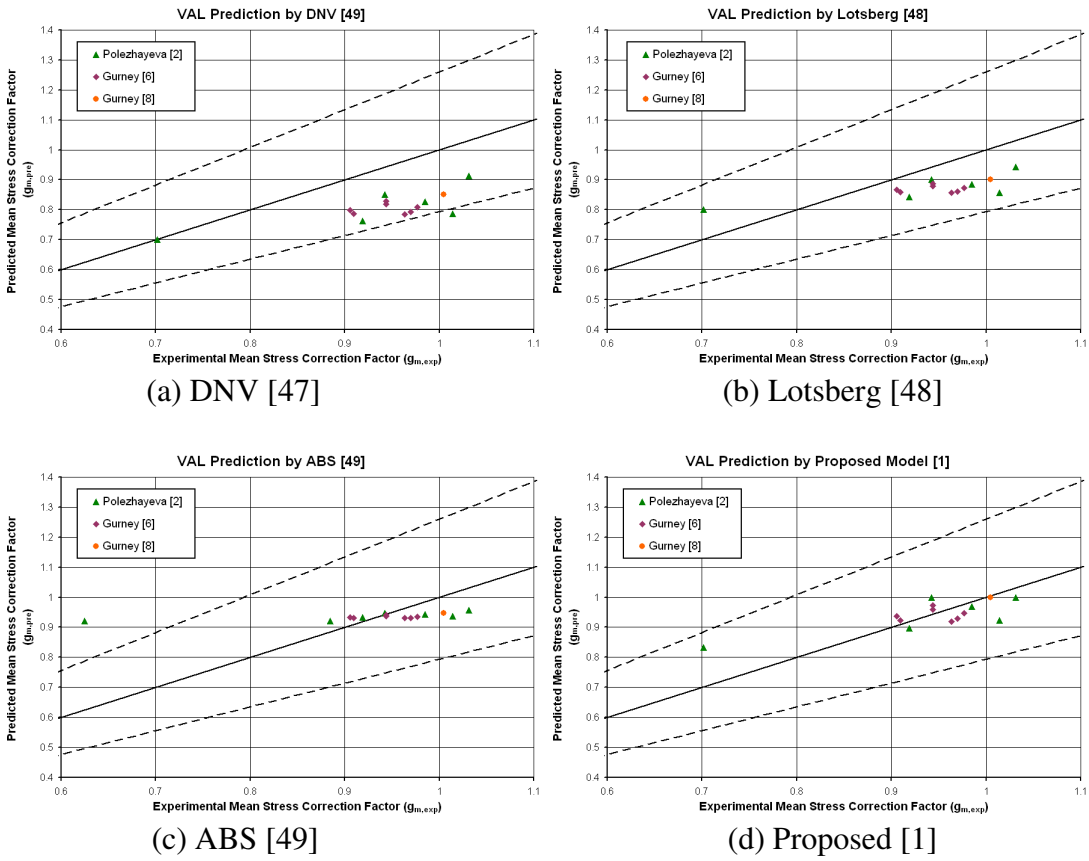

Figure 52: Comparison of the Predicted to the Experimental Mean Stress Correction Factors under Variable Amplitude Loading

3.3 CASE STUDY

To further compare the above fatigue models, the DNV, the Lotsberg, the ABS and the proposed models were used to perform a fatigue analysis of a test case. This test case involved a typical naval vessel subjected to a spectral loading condition. In the fatigue analysis, the response RAOs and the input wave spectra were combined with the hot pot stresses evaluated for unit panel load cases. The response RAOs were obtained through a hydrodynamics analysis using 800 panels on the wet surface of the ship hull. The hot spot stresses due to the unit panel pressure load cases were generated using a top-down approach, in which a global finite element analysis was first conducted using a model shown in Figure 53 and the displacement results from global analysis were then prescribed to a detailed local model (Figure 54) to obtain more accurate local stresses.

In order to reveal the influence of the mean stress levels on the predicted fatigue life, four different mean stress values were considered, including negative, zero and positive mean stresses as indicated in Table 17. As expected all mean stress models predicted shorter fatigue lives with the increase of the mean stress level. This trend is due to the modification to the compressive part of the fatigue cycle. When the mean stress is further increased so that the fatigue cycle is predominantly tensile, all mean stress correction models produced very similar results as indicated in the last column in Table 17. The results also showed that the proposed model predicted the shortest fatigue initiation lives and therefore was the most conservative, while the DNV and the Lotsberg models were the least conservative.

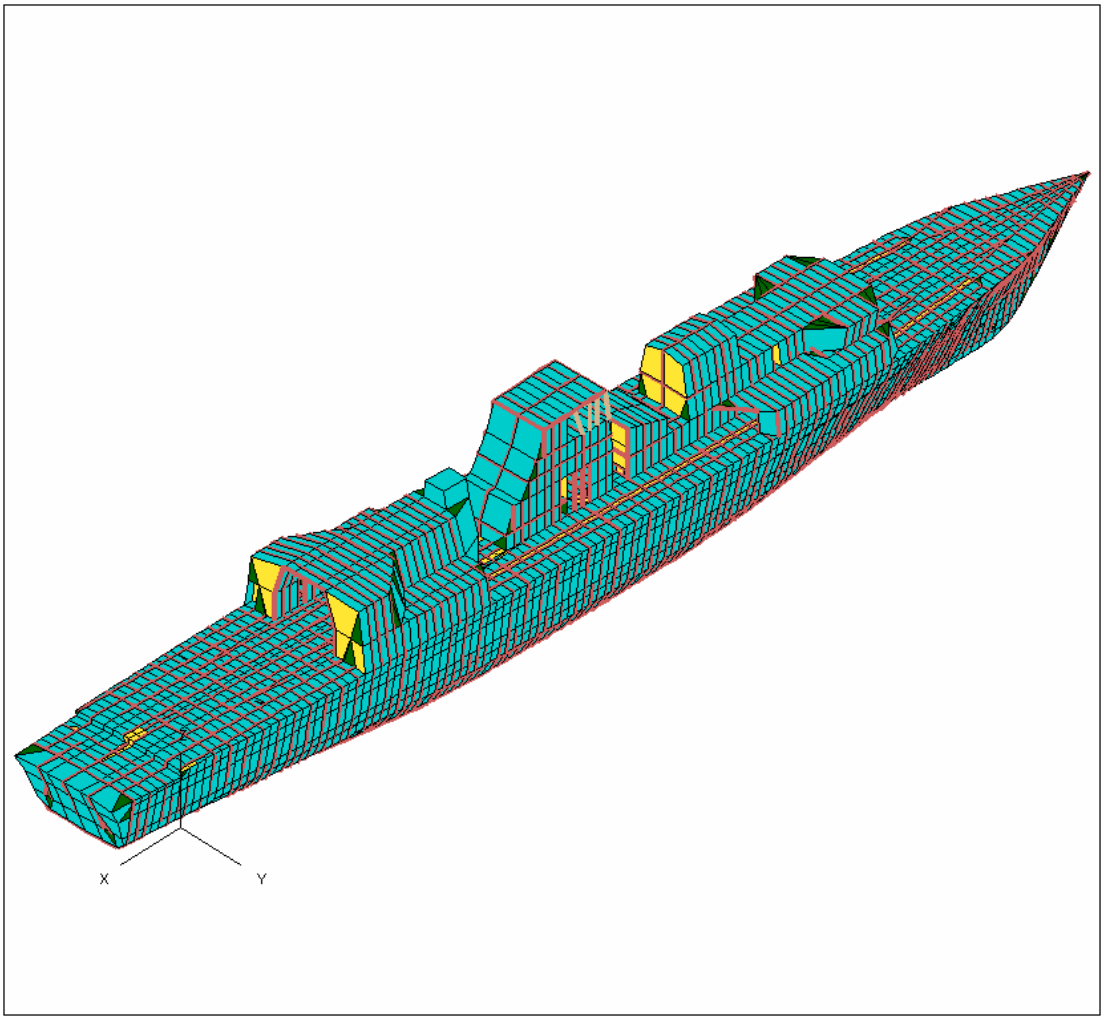

Figure 53: Global Finite Element Model of a Typical Naval Vessel used in the Case Study

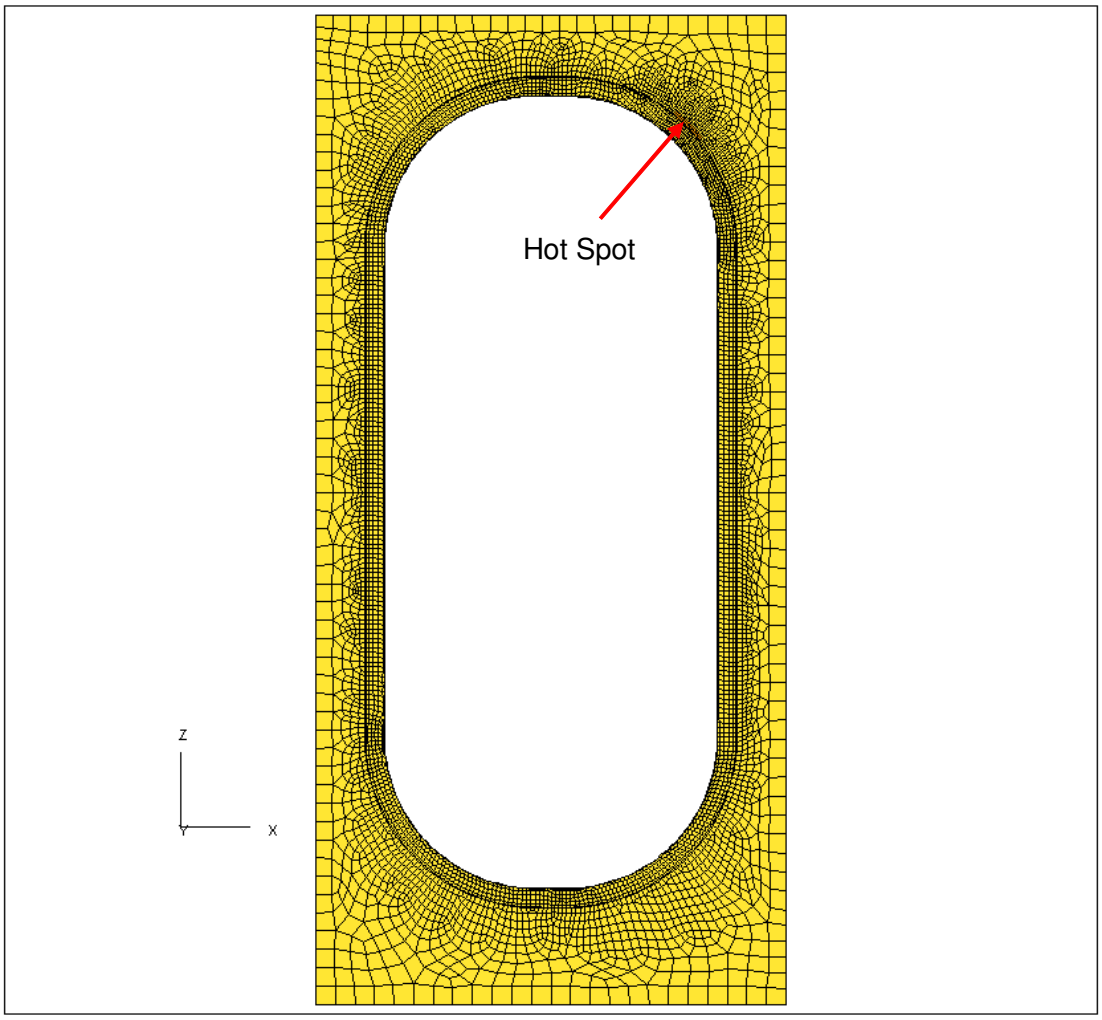

Figure 54: Local Finite Element Model of the Hot Spot used in the Case Study

Table 17: Fatigue Life Predicted by Different Mean Stress Models for Various Mean Stress Levels

Model	Fatigue Life for Initiation (hours)			
	σ_{mean} = -3.93 MPa	σ_{mean} = 0.00 MPa	σ_{mean} = 4.00 MPa	σ_{mean} = 21.07 MPa
DNV [47]	2.278297×10^5	1.877439×10^5	1.551010×10^5	1.171646×10^5
Lotsberg [48]	1.785207×10^5	1.581323×10^5	1.398415×10^5	1.165387×10^5
ABS [49]	1.448191×10^5	1.356008×10^5	1.272397×10^5	1.159090×10^5
Proposed [1]	1.410285×10^5	1.152420×10^5	1.152420×10^5	1.152420×10^5

4.0 SUMMARY, CONCLUSIONS AND RECOMMENDATIONS

4.1 SUMMARY AND CONCLUSIONS

The mean stress is an important component of loading history and fatigue of ship hull structural details. This is especially true in welded details, where tensile residual stress at a hot spot is very large and close to the yield stress, which might reduce the fatigue life of structural components. However, there is a lack of commonality between different approaches in fatigue analysis and design codes and standards when dealing with mean stress. Therefore, the objectives of this work were to validate the models adopted in the various approaches, to seek to harmonize these approaches across the codes and to develop an appropriate methodology for assessing the effects of mean stress. These objectives were accomplished through a review the available data on the effects of mean stress on fatigue strength and the analyses the available fatigue data in order to develop an appropriate methodology for the assessment of the mean stress effects in fatigue analysis for marine applications. The following conclusions are drawn from [1] and the present work:

1. In welded details, tensile residual stress at a hot spot is very large and close to the yield stress. The compressive part of a fatigue cycle is only partly damaging, but down to a stress ratio of $R = -1$, the compressive part provides no significant benefit to the fatigue strength. Under a fully compressive applied stress range, the enhancement factor on fatigue strength varied widely from 1.17 to 1.48. There is not much data on the benefit of partly compressive cycles where the compressive part of the cycle is larger than the tensile part (i.e. stress ratios between $R = -1$ and $R = -\infty$), as shown by the lack of entries in the fatigue test database. However there is an indication that the mean stress influences the fatigue strength of welded joints under variable amplitude loading typical for ships.

2. Static loading on a ship structure, induced either by water pressure before service such as a tank test and ballasting, or by static cargo or ballast pressure during laden or ballast voyages, cause relatively high static mean hot spot stresses at welded joints, compared with cyclic loadings induced by waves during service. Due to these static pre-loadings, the initial tensile residual stresses at welded joints and/or flame cut edges, where fatigue strength is of concern(in most cases, where stress concentration occurs), are expected to be shaken-down to a great extent by the elasto-plastic deformation behaviour of the material. However, not every fatigue prone welded joint in ship is subjected to tank test and ballasting static loading, so residual stress relaxation due to these loads is not guaranteed. On the other hand, static loads due to cargo or ballast pressure are unavoidable.

3. The literature review revealed that initial residual stress relaxation occurs mostly during the application of first half cycle of positive stress. According to the limited experimental data, the relaxation of residual stress is negligible if the initial (static) applied positive hot spot stress is below $0.6\sigma_y$. Analysis of experimental data showed that the average reduction in residual stress is 60%, with a lower limit of reduction of 20%, after an application of a hot spot

stress equal to yield stress of material. Based on the literature review, it is conservative to assume that no relaxation occurs after application of fully compressive stresses. There is not enough data to analyse residual stress relaxation after the application of partly compressive stress cycles.

4. A new fatigue model is proposed based on the current investigation and literature search. It is assumed in this model that there is no fatigue enhancement when the compressive part of the fatigue cycle is smaller than the tensile part (i.e. when $R > -1$). The fatigue enhancement factor is proposed in this model to increase from 1.0 for $R = -1$ (50% compression) to 1.2 for $R = -\infty$ (100% compression) in the loading history. It was shown that the proposed model is more conservative at predicting the mean stress effect than three different Class Society models, when compared to fatigue test results from various sources.

4.2 RECOMMENDATIONS

The following are recommendations for future work:

1. Investigate the benefit of partly compressive cycles where the stress ratio is between $R = -1$ and $R = -\infty$ and fatigue data are lacking.

2. Develop a model for residual stress relaxation as a function of the applied stress range, stress ratio and initial residual stress.

5.0 REFERENCE

[1] Polezhayeva, H. *Literature Review on Mean Stress Effect on Fatigue Strength of Welded Joints*. MPD/10/06, Lloyd's Register, November 2010.

[2] Polezhayeva, H. *Fatigue Testing of Welded Panels*. MPD/10/05, Lloyd's Register, November 2010.

[3] Maddox, S.J. "Influence of Tensile Residual Stresses on the Fatigue Behaviour of Welded Joints in Steel." *Residual Stress Effects in Fatigue*, ASTM STP 776 (1982): 63-96.

[4] Maddox, S.J. *The Influence of Residual Stress on the Fatigue Behaviour of Al-Zn-Mg Alloy Fillet Welds*. University of Southampton.

[5] Tilly, G.P. "Fatigue Review. Fatigue of Land-Based Structures." *International Journal of Fatigue*, Vol. 7 No. 2 (1985): 67-78.

[6] Gurney, T.R. "Fatigue Tests on Fillet Welded Joints under Variable Amplitude Loading." *TWI Research Report*, No. 293/1985 (1985).

[7] Niemi, E.J. "Fatigue Tests on Butt and Fillet Welded Joints under Variable Amplitude Loading." *Fatigue of Welded Constructions*, (April 1985).

[8] Gurney, T.R. "Fatigue Tests on Fillet Welded Joints in Steel under Simulated Wide Band Type Loading." *TWI Research Report*, No. 365/1988 (1988).

[9] Gurney, T.R. "The Influence of Mean and Residual Stresses on Fatigue Strength of Welded Joints under Variable Amplitude Loading – Some Exploratory Tests." *TWI Research Report*, No. 464/1992 (1992).

[10] Rörup, J. and Petershagen, H. "The Effect of Compression Mean Stresses on the Fatigue Strength of Welded Structures." *Welding in the World*, Vol. 44, 5 (2000).

[11] Rörup, J. and Fricke, W. "Mean Compressive Stresses – Experimental and Theoretical Investigations into the Influence on the Fatigue Strength of Welded Structures." *Doc. XIII-2007-04* (March 2004).

[12] Marquis, G.B. and Mikkola, T.P.J. "Effect of Mean Stress Changes on the Fatigue Strength of Spectrum Loaded Welds." *Practical Design of Ships and Other Floating Structures Proceedings*, (2001).

[13] Sonsino, C.M., Maddox, S.J. and Hobbacher, A. "Fatigue Life Assessment of Welded Joints under Variable Amplitude Loading – State of Present Knowledge and Recommendations for Fatigue Design Regulations." (2003): 87-102.

[14] Kassner, M. and Krebs, J. "Influence of Welding Residual Stresses and Notch Effect on Fatigue Data for Welded Joints and Components." *International Institute of Welding*, XV-1255r1-07, XIII-2171r1-07 (2007).

[15] Hobbacher, A. "Recommendations for Fatigue Design of Welded Joints and Components." *IIW-XIII/XV-1254r1-07* (May 2007).

[16] Heo, J-H., Kang, J-K, Kim, K-S and Urm, H-S. "A Study on the Fatigue under Combined Tensile and Compressive Mean Stresses in Ship Structure." *PRADS* (2007).

[17] Bousseau, M. and Millot, T. "Initiation and Propagation of Cracks in Welded Joints Subject to Compression Stress." *Doc.XIII-2237-08* (2008).

[18] Gadouini, H., Nadot, Y. and Rebours, C. "Influence of Mean Stress on the Multiaxial Fatigue Behaviour of Defective Materials." *International Journal of Fatigue*, Vol. 30 (2008): 1623-1633.

[19] Colin, J., Fatemi, A. and Taheri, S. "Fatigue Behaviour of Stainless Steel 304L Including Strain Hardening, Prestraining, and Mean Stress Effects." *Journal of Engineering Materials and Technology*, Vol. 132 (April 2008): 021008-1-021008-13.

[20] Smith, K.N., Watson, P. and Topper, T.H. "A Stress-Strain Function for the Fatigue of Metals." *J. Mater.*, Vol. 5 (1970): 767-778.

[21] Aid, A., Amrouche, A., Bachir Bouiadjra, B., Benguediab, M. and Mesmacque, G. "Fatigue Life Prediction under Variable Loading Based on a New Damage Model." *Materials and Design*, Vol. 32 (2011): 183-191.

[22] FPSO JIP – Fatigue Capacity. "Fatigue Test of Typical Weld Joints (A Proposal of S-N Diagrams for Welded Ship Structure)." *Hyundai Heavy Industries. Co., Ltd.* (2000.4).

[23] Lotsberg, I. and Landet, E. "Fatigue Capacity of Side Longitudinals in Floating Structures." *OMAE-FPSO 2004*, Houston, USA (2004).

[24] Borgren, J. and Lopez Martinez, L. "Spectrum Fatigue Testing and Residual Stress Measurements on Non-Load Carrying Fillet Welded Test Specimens." *Fatigue under Spectrum Loading and Corrosive Environments*, Warley, UK, EMAS (1993).

[25] Maddox, S.J. "Fracture Mechanics Applied to Fatigue in Welded Structures." *Welding Institute Conference on Fatigue of Welded Structures*, Brighton, England (1970): 73-96.

[26] Nitschke-Pagel, Th. "Residual Stresses and Fatigue Behaviour of Welded High Strength Steels." *Diss. TU Braunschweig* (1994).

[27] Blom, A.F. "Spectrum Fatigue Behaviour of Welded Joints." *International Journal of Fatigue*, Vol. 17 (1995): 485-491.

[28] Lopez Martinez, L. Lin, R., Want, D. and Blom, A.F. "Investigation of Residual Stresses in As-Welded and TIG-Dressed Specimens Subjected to Static/Spectrum Loading." *Proceedings of the North European Engineering and Science Conference (NESC): Welded High-Strength Steel Structures*, Stockholm, Sweden (Edited by A.F. Blom), EMAS Publishing, London, UK (1997).

[29] Iida, K., Yamamoto, S. and Takanashi, M. "Residual Stress Relaxation by Reversed Loading." *Welding in the World/le Soudage dans le Monde*, Vol. 39 (1997): 138-144.

[30] Iida, K. and Takanashi, M. "Relaxation of Welding Residual Stresses by Reversed and Repeated Loadings." *Welding in the World/le Soudage dans le Monde*, Vol. 41 (1998): 138-144.

[31] Takanashi, M., Kamata, K. and Kunihiro, I. "Relaxation Behaviour of Welding Residual Stresses by Fatigue Loading in smooth Longitudinal Butt Welded Joints." *Welding World*, Vol. 44 (2000): 28-34.

[32] Nitschke-Pagel, Th. and Wohlfahrt, H. "Residual Stress Relaxation in Welded High Strength Steels under Different Loading Conditions." *Proceedings of the 6th International Conference on Residual Stresses: ICRS-6*, Oxford, UK (2000): 1495-1502.

[33] Lachmann, C., Nitschke-Pagel, Th. and Wohlfahrt, H. "Characterisation of Residual Stress Relaxation in Fatigue Loaded Welded Joints by X-Ray Diffraction and Barkhausen Noise Method." *ECRS 5, Proceedings of the 5th European Conference on Residual Stresses*, Delft-Noordwijkerhout, the Netherlands, *Material Science Forum*, Vol. 47 (2000): 374-379.

[34] Han, S.T. Lee and Shin, B. "Residual Stress Relaxation of Welded Steel Components under Cyclic Load." *Material Technology*, Vol. 73 (2002): 414-420.

[35] Dattoma, V., De Giorgi, M. and Nobile, R. "Numerical Evaluation of Residual Stress Relaxation by Cyclic Load." *Journal of Strain Analysis for Engineering Design*, Vol. 39 (2004): 663-672.

[36] Barsoum, Z. and Gustafsson, M. "Spectrum Fatigue of High Strength Steel Joints Welded with Low Temperature Transformation Consumables." *2nd International Conference on Fatigue Design*, Senlis, France (2007).

[37] Farajian-Sohi, M., Nitschke-Pagel, Th. and Dilger, K. "Residual Stress Relaxation of Quasistatically and Cyclically Loaded Welded High Strength Steels." *XIII-2219-08* (2008).

[38] Farajian, M., Nitschke-Pagel, Th. and Dilger, K. "Mechanisms of Residual Stress Relaxation and Redistribution in Welded High Strength Steel Specimens under Mechanical Loading." *XIII-2275-09* (2009).

[39] Das, S. "Exact Mapping of Residual Stress in Ship Hull Structures (First Quarterly Report on Literature Review)." *SSC Project SR-1456* (2010).

[40] Lorentzen, T. and Ibsø, J.B. "Neutron Diffraction Measurements of Residual Strains in Offshore Welds." *Material Science and Engineering A*, Vol. A197 (1995): 209-214.

[41] Gao, H., Guo, H., Blackburn, J.M. and Hendricks, R.W. "Determination of Residual Stress by X-Ray Diffraction in HSLA-100 Steel Weldments." *Fifth International Conference on Residual Stress*, Linkoping, Sweden: Linkopings Universitet (1997): 320-325.

[42] Hu, S.Z. and Jiang, L. "A Finite Element Simulation of the Test Procedure of Stiffened Panels." *Marine Structures*, No. 11 (1998): 75-99.

[43] Rörup, J. "Mean Compressive Stresses – Experimental and Theoretical Investigations into their Influence on the Fatigue Strength of Welded Structures." *Journal of Strain Analysis for Engineering Design 40*, No. 7 (2005): 631-642.

[44] Ayala-Uraga, E. and Moan, T. "Time-Variant Reliability Assessment of FPSO Hull Girder with Long Cracks." *Journal of Offshore Mechanics and Arctic Engineering* 129 (May 2007): 81-89.

[45] Bannantine, J.A., Comer, J.J. and Handrock, J.L. *Fundamentals of Metal Fatigue Analysis*. Prentice Hall, Upper Saddle River, N.J. (1990).

[46] Lee, Y-L. *Fatigue Testing and Analysis: Theory and Practice*. Elsevier Butterworth-Heinemann, Amsterdam; Boston. (2005).

[47] *Fatigue Design of Offshore Steel Structures*. Recommended Practice DNV-RP-C203. (April 2010).

[48] Lotsberg, I. "Assessment of Fatigue Capacity in the New Bulk Carrier and Tanker Rules." *Marine Structures*, Vol. 19 (2006): 83-96.

SHIP STRUCTURE COMMITTEE LIAISON MEMBERS

LIAISON MEMBERS

American Society of Naval Engineers	Captain Dennis K. Kruse (USN Ret.)
Bath Iron Works	Mr. Steve Tarpy
Colorado School of Mines	Dr. Stephen Liu
Edison Welding Institute	Mr. Rich Green
International Maritime Organization	Mr. Igor Ponomarev
Int'l Ship and Offshore Structure Congress	Dr. Alaa Mansour
INTERTANKO	Mr. Dragos Rauta
Massachusetts Institute of Technology	
Memorial University of Newfoundland	Dr. M. R. Haddara
National Cargo Bureau	Captain Jim McNamara
National Transportation Safety Board - OMS	Dr. Jack Spencer
Office of Naval Research	Dr. Yapa Rajapaksie
Oil Companies International Maritime Forum	Mr. Phillip Murphy
Samsung Heavy Industries, Inc.	Dr. Satish Kumar
United States Coast Guard Academy	Commander Kurt Colella
United States Merchant Marine Academy	William Caliendo / Peter Web
United States Naval Academy	Dr. Ramswar Bhattacharyya
University of British Columbia	Dr. S. Calisal
University of California Berkeley	Dr. Robert Bea
Univ. of Houston - Composites Eng & Appl.	
University of Maryland	Dr. Bilal Ayyub
University of Michigan	Dr. Michael Bernitsas
Virginia Polytechnic and State Institute	Dr. Alan Brown
Webb Institute	Prof. Roger Compton

RECENT SHIP STRUCTURE COMMITTEE PUBLICATIONS

Ship Structure Committee Publications on the Web - All reports from SSC 1 to current are available to be downloaded from the Ship Structure Committee Web Site at URL: http://www.shipstructure.org
SSC 445 – SSC 393 are available on the SSC CD-ROM Library. Visit the National Technical Information Service (NTIS) Web Site for ordering hard copies of all SSC research reports at URL: http://www.ntis.gov

SSC Report Number	Report Bibliography
SSC 465	Predictive Modeling Impact of Ice on Ship and Offshore Structures Bueno A. 2012
SSC 464	Design and Detailing for High Speed Aluminum Vessels Design Guide and Training Mish, Wh Jr., Lynch T., Hesse E., Kulis J., Wilde J., Snyder Z., Ruiz F. 2012
SSC 463	Marine Composites NDE, Inspection Techniques for Marine Composite Construction Greene, E 2012
SSC 462	Review of Current Practices of Fracture Repair Procedures for Ship Structures Wang, G, Khoo, E., ABS Corporate Technology 2012
SSC 461	Structural Challenges Faced By Arctic Ships, Kendrick A., Daley C. 2011
SSC 460	Effect of Welded Properties on Aluminum Structures, Sensharma P., Collette M., Harrington J. 2011
SSC 459	Reliability-Based Performance Assessment of Damaged Ships, Sun F., Pu Y., Chan H., Dow R.S., Shahid M., Das P.K. 2011
SSC 458	Exact Mapping of Residual Stress in Ship Hull Structures by Use of Neutron Diffraction Das. S. Kenno S. 2009
SSC 457	Investigation of Plastic Limit States for Design of Ship Hull Structures, Daley C., Hermanski G. 2009
SSC 456	Buckling Collapse Testing on Friction Stir Welded Aluminum Stiffened Plate Structures, Paik J.K. 2009
SSC 455	Feasibility, Conceptual Design and Optimization of a Large Composite Hybrid Hull, Braun D., Pejcic M. 2008
SSC 454	Ultimate Strength and Optimization of Aluminum Extrusions, Collette M., Wang C. 2008
SSC 453	Welding Distortion Analysis Of Hull Blocks Using Equivalent Load Method Based On Inherent Strain, Jang C.D. 2008
SSC 452	Aluminum Structure Design and Fabrication Guide, Sielski R.A. 2007